Korean J. Chem. Eng., 40(12), 3106-3129 (2023)
DOI: 10.1007/s11814-023-1578-9

pISSN: 0256-1115
eISSN: 1975-7220

Multi-functional hydrogel electrodes for emerging electronic and robotic applications

Jongkuk Ko†

Department of Chemical and Biological Engineering, Gachon University, Gyeonggi-do 13120, Korea
(*Received 20 August 2023 • Revised 10 September 2023 • Accepted 19 September 2023*)

Abstract−Functional hydrogels have emerged as a new class of electronic and robotic materials owing to their unique features. The development of high-performance conductive hydrogels with diverse functionalities has expected to result in important breakthroughs in the fields of electronics and robotics. In this review, the current advances in the fabrication of multi-functional hydrogel electrodes for both electronic and robotic applications are presented. Four different types of hydrogel electrodes are considered depending on their fabrication methods: i) ionically conductive hydrogel, ii) conductive polymer-based hydrogel, iii) conductive nanocomposite hydrogel, and iv) conductive layer-coated hydrogel. Their distinguishing attributes compared to those of other types of soft electrodes, as well as the current challenges for each type of hydrogel electrodes, are discussed. This review also illustrates the recent advances in electronic and robotic applications using hydrogel electrodes. Finally, future directions for capturing these opportunities and overcoming the challenges of conductive hydrogels are discussed.

Keywords: Hydrogel Electrode, Electrode Fabrication, Electronics, Robotics

INTRODUCTION

The introduction of various soft functional materials has shown great promise for revolutionizing the electronic [1-6] and robotic [2,7-11] fields for a wide range of human-friendly applications. Moreover, the development of new technologies to impart electrical properties to functional soft materials has played a key role in the development of new classes of electronic and robotic devices, overcoming the intrinsic limitations of conventional electronics and robotics (e.g., difficulties in simultaneously achieving high mechanical and electrical properties and difficulties in incorporating multiple functionalities). Therefore, tremendous research efforts have been dedicated to developing new soft electronic materials and their fabrication methods based on synthesizing new conductive soft materials, or integrating soft materials (e.g., PI, PET, rubber, and silicone) with conductive materials (e.g., CNT, graphene, liquid metal, Au, and Ag) [1-6,12-25]; however despite these significant advances, realizing electronic and robotic devices with outstanding electrical properties (e.g., electrical conductivity), favorable mechanical properties (e.g., tissue-like softness, stretchability, and toughness), and multifunctionalities (e.g., self-healing, biocompatibility/degradability, and stimuli-responsiveness) remains a challenge. Thus, it is highly desirable to develop a new class of versatile soft electronic materials for the further advancement of next-generation electronic and robotic applications.

Hydrogels exhibit distinctive attributes such as high water content, stretchability, tissue-like softness, permeability to various molecules, stimuli-responsiveness, and chemical diversity, similar to those of biological tissues. In particular, hydrogels possess the versatility to integrate all properties and functionalities into a single material, which is difficult to achieve using other types of soft materials. Despite the unique properties of hydrogels, it has been challenging to endow hydrogels with high electrical properties without affecting their unique features because their high liquid (i.e., water) content and significantly hydrated surface layers. New versatile methods for imparting excellent electrical properties to a variety of functional hydrogels will pave the way for breakthroughs in emerging electronic and robotic applications.

There have been lots of studies to fabricate conductive hydrogels based on four different strategies as illustrated in Fig. 1: i) embedding mobile ions, ii) using conductive polymer, iii) incorporating conductive fillers inside hydrogel matrix, and iv) coating conductive materials on hydrogel surfaces. Embedding mobile ions in the water phase of hydrogels is a facile method for employing hydrogels in numerous electronic and robotic applications; however, their electrical conductivity is intrinsically limited. Conductive polymers can provide favorable mechanical properties with high electrical conductivities. However, the number of conductive polymers that are compatible with hydrogels and their degrees of electrical conductivity are limited. Incorporating conductive components into a hydrogel matrix has a been widely studied strategy for preparing conductive hydrogels, demonstrating promising applications in the electronic and robotic fields based on their high electrical conductivity. However, large amounts of conductive components inside the hydrogel matrix, which are necessary to achieve high electrical conductivity, lead to undesirable mechanical properties and functionalities. Coating conductive materials on a hydrogel surface can provide the highest electrical conductivity based on its densified conductive layer; however there have been insufficient studies on this method. Further advances in conductive hydrogels with favorable mechanical properties and functionalities are required.

Owing to the promising opportunities for conductive hydrogels,

†To whom correspondence should be addressed.
E-mail: kojk@gachon.ac.kr

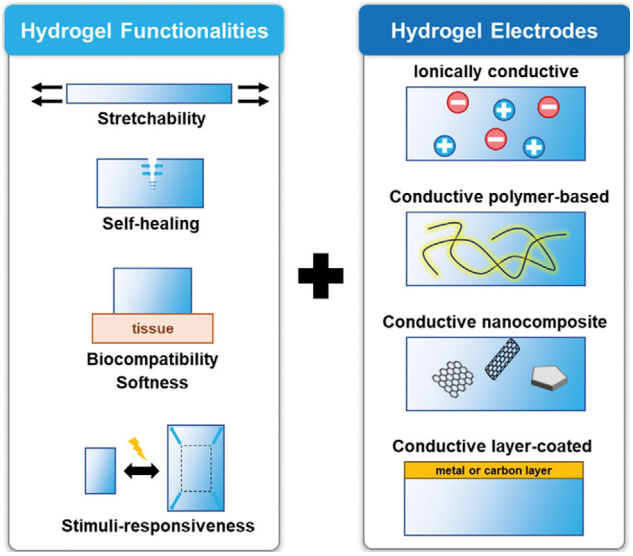

Fig. 1. Schematic illustration of functionalities of hydrogel and different types of conductive hydrogels depending on the fabrication methods for multi-functional hydrogel electrodes for electronic and robotic applications.

a series of reviews on conductive hydrogels have been recently reported [26-33]. However, most previous reviews lack a description of the coating methods and their wide range of available applications despite their promising opportunity to develop high-performance hydrogel electrodes with diverse functionalities. In this review, current approaches for constructing multi-functional hydrogel electrodes for both electronic and robotic applications are presented. First, several important properties and functionalities of the hydrogels are introduced and compared with those of other types of soft materials. Second, four different types of methods for endowing hydrogels with electrical conductivity are described. Additionally, the drawbacks and challenges of each method are discussed. Third, hydrogel-based electronic and robotic applications are presented, demonstrating new electronic and robotic devices that cannot be realized using conventional soft electrodes. Finally, essential roles and perspectives of multi-functional hydrogel electrodes in those fields are discussed.

UNIQUE PROPERTIES OF HYDROGELS

Hydrogels are a special class of soft materials composed of hydrophilic three-dimensional (3D) network structures of solid and dispersed liquid phases (water). Typically, hydrogels are composed of elastic polymeric chains crosslinked in 3D structures that are swollen by a large amount of water. Numerous types of 3D network structures of polymers with different chemical structures are available, resulting in a variety of tunable properties. Therefore, hydrogels can exhibit a wide range of chemical diversity by changing the configuration of their polymeric network structures, which can be controlled by changing various parameters, including the types of monomers, composition of monomers, nature of crosslinks, crosslink density, and concentration of the polymeric network. Such a wide chemical diversity in hydrogels enables them to possess various unique properties, including stretchability, tissue-like softness, transparency, adhesiveness, stimuli-responsiveness, and self-healing, which are difficult to observe in other types of soft materials [26,27,31-34].

1. Mechanical Properties

The intrinsic nature of hydrogels allows for favorable mechanical properties, such as a high degree of stretchability and a wide range of elastic moduli [26,27,32,34-37]. A three-dimensional elastic polymeric network with a high water content of hydrogel enables stretching of its structure, typically by over a few hundred percent (Fig. 2(a)). In addition, the elastic modulus of the hydrogels can be readily modulated from a few kPa to a few MPa by controlling the configuration of the 3D network structures, including the chemical structures, type/density of crosslinks, and polymer concentration. The superior softness and stretchability of hydrogels play important roles in the development of various types of hydrogel-based electronics and robotics. Considering that the elastic modulus of soft tissues ranges from ~ a few kPa (e.g., brain tissue) to ~ a few MPa (e.g., muscle) [38], hydrogels can easily match the softness of most soft tissues for biological tissue-interfaced applications, which is difficult to achieve with other types of soft materials.

Despite the promising mechanical properties of hydrogels that mimic those of soft biological tissues, there are stiffer biological tissues which are still challenging to realize with synthetic materials. For example, tendon shows strong and tough mechanical properties simultaneously (i.e., elastic modulus ~1 GPa, tensile strength ~100 MPa) [38], and because of the conflicting mechanical properties between stiffness and toughness, soft materials with a high degree of stiffness and toughness remain challenging tasks. Specifically, increasing the crosslink density in hydrogels, which is a conventional approach for enhancing their stiffness, leads to brittle structures.

Several design principles and strategies have been suggested to address the aforementioned challenges, including the use of two different types of polymer networks (double networks), reinforcement by incorporated fibers/fabrics, alignment of microstructures, and incorporation of nanocomposites [39-44]. Rational molecular and structural design of hydrogels results in considerably enhanced mechanical properties. For example, a nanocomposite hydrogel achieved a significantly high modulus (>100 MPa) with 45% water content as shown in Fig. 2(b) [39-44]. However, there is still a lack of research on realizing hydrogels mimicking the superior mechanical properties of biological tissues, such as simultaneously high strength and toughness.

Recently, a facile approach to prepare hydrogels combining high degrees of stiffness and toughness at the same time was suggested by inducing considerable chain entanglement in the hydrogel matrix [45,46]. When the number of entanglements significantly increased compared to that of crosslinks in the hydrogel matrix, physical chain entanglement could effectively transmit stress, dissipating mechanical energy without sacrificing the stiffness of the materials. Based on the high density of chain entanglement, polyacrylamide (PAAm) and protein hydrogels can achieve a few orders of magnitudes higher stiffness and toughness, overcoming the trade-off between these mechanical properties.

2. Adhesion Properties

Despite the large number of hydrophilic groups present in hydro-

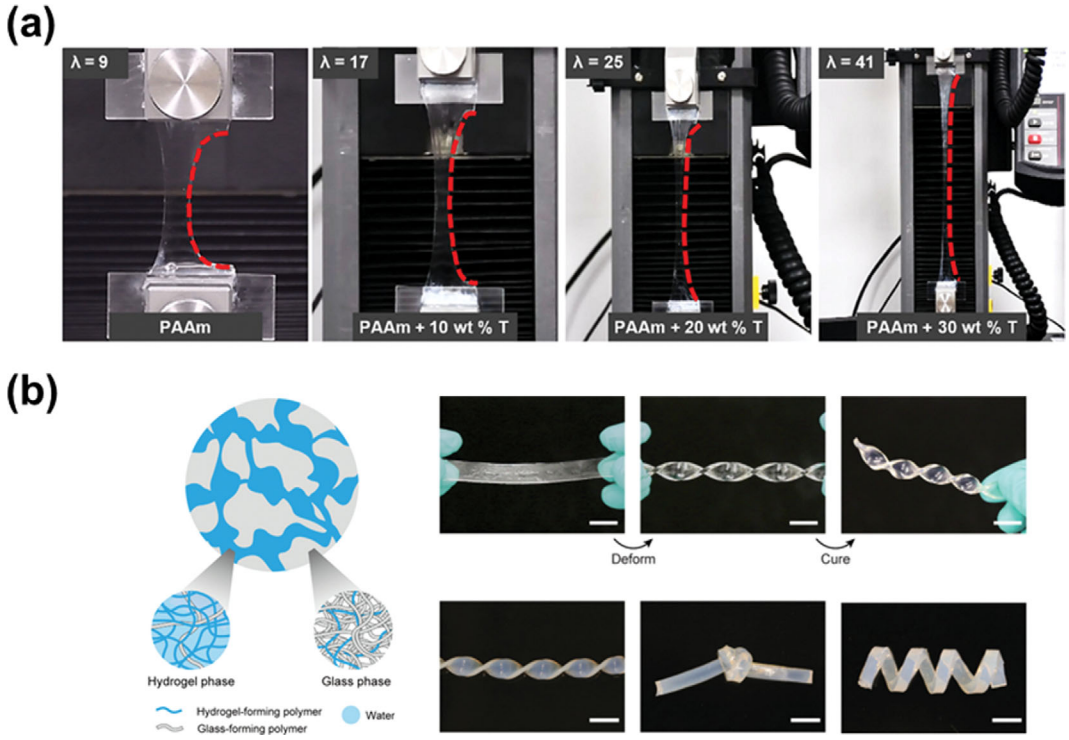

Fig. 2. Unique mechanical properties of hydrogel. (a) Trehalose modified PAAm hydrogel showing high strength and stretchability. Adapted from ref. [37] under the terms of the CC BY-NC, Creative Commons Attribution NonCommercial License 4.0 (https://creativecommons.org/licenses/by-nc/4.0), copyright 2022 AAAS. (b) Poly(methyl methacrylate)-poly(acrylic acid) nanocomposite hydrogel showing high stiffness and toughness. Adapted from ref. [44] under the terms of the CC BY-NC, Creative Commons Attribution NonCommercial License 4.0 (https://creativecommons.org/licenses/by-nc/4.0), copyright 2022 PNAS.

gels, the intrinsic nature of hydrogels (i.e., high water content and significantly hydrated surface layer) seriously restricts the formation of strong bonds with other types of non-porous solid materials. (e.g., polymers, metals, and elastomers) However, over the last decade, a series of studies demonstrated the robust adhesion of hydrogels to various synthetic and biological materials based on covalent binding and the energy-dissipation mechanisms. Based on the interfacial adhesion principle, Yuk et al. reported interfacial toughness of over 1,000 J m^{-2} between hydrogel and various solids (e.g., glass, silicon, ceramics, titanium and aluminum) [47]. First, after a functional silane (i.e., 3-(trimethoxysilyl) propyl methacrylate (TMSPMA)) was applied to the target substrate, networks of the polymer (that is PAAm or polyethylene glycol diacrylate (PEGDA)) was covalently bonded to silane-modified surfaces. Based on this chemical anchorage and energy dissipation of the stretchable hydrogel matrix, extraordinarily robust adhesion of the hydrogel to diverse solids was achieved. Several different types of strategies, including oxygen inhibition-based surface activation of elastomers and hydrogel polymer grafting, silane coupling agent-based dissimilar polymer network bonding, and cyanoacrylate-based instant tough bonding methods [48-52], have also been suggested to improve interfacial adhesion (Fig. 3(a)).

Moreover, strong and rapid adhesion of the hydrogel to wet biological tissues was demonstrated based on the architecture of dry double-sided tape (DST) with a dry-crosslinking mechanism [53-55]. The tissue adhesive (DST) was fabricated using a biopolymer (gelatin or chitosan) and N-hydroxysuccinimide (NHS) ester-grafted poly(acrylic acid) in the dried state. When DST contacts wet tissue, it become swollen and crosslinked by the rapid absorption of the interfacial water layer on the tissue surface. The swollen DST can form instant intermolecular crosslinks on the dried tissue surface, resulting in the formation of intermolecular bonds (i.e., hydrogen bonds and electrostatic interactions) by the carboxylic acid groups in the hydrogel. Moreover, NHS ester groups in hydrogel formed additional covalent bonding with various primary amines group on tissue surface, demonstrating high fracture energy (>1,000 J m^{-2}).

Functional hydrogels have been successfully integrated with various materials with arbitrary shapes based on the aforementioned methods. Hydrogel-integrated composites can be used in new applications by combining the functions of hydrogels and integrated materials.

3. Biocompatibility and Biodegradability

Biocompatibility is the capability of materials to sustain their structure and function when interfaced with biological tissues or cells, without foreign body responses or undesirable effects [56-58]. Hydrogels can be classified into two different types according to their source: natural and synthetic polymers. Naturally originated hydrogels prepared based on collagen, gelatin, hyaluronate, cellulose, alginate, agarose, or chitosan, which are easily found in nature and components for human body, have demonstrated favorable biocompatibility [26,56-64]. In addition, various synthetic polymers

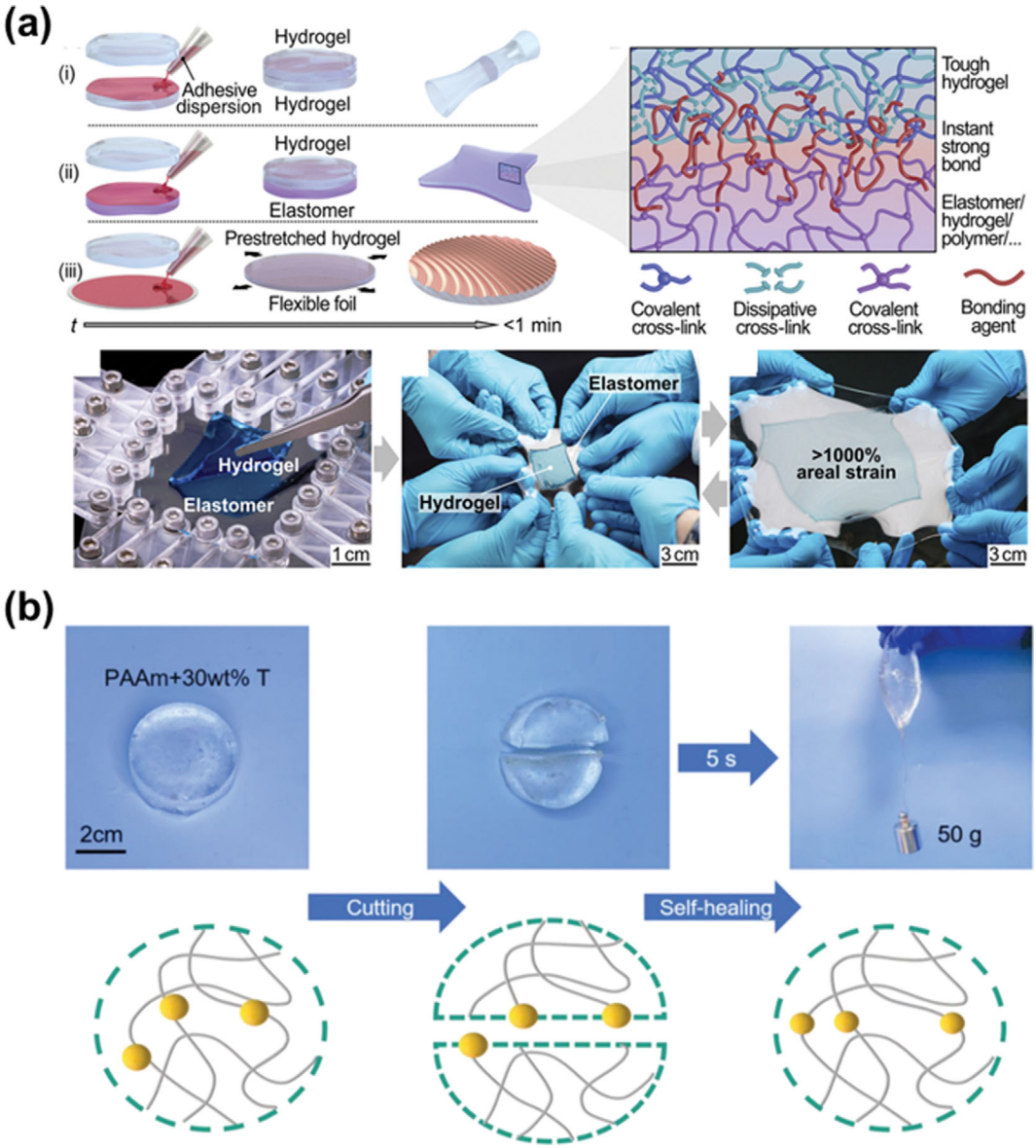

Fig. 3. Unique properties of hydrogel. (a) An adhesive-assisted strong adhesion of hydrogel with diverse materials. Adapted from ref. [49] under the terms of the CC BY-NC, Creative Commons Attribution NonCommercial License 4.0 (https://creativecommons.org/licenses/by-nc/4.0), copyright 2017 AAAS. (b) Trehalose modified PAAm hydrogel showing rapid self-healing capability by hydrogen bonds. Adapted from ref. [37] under the terms of the CC BY-NC, Creative Commons Attribution NonCommercial License 4.0 (https://creativecommons.org/licenses/by-nc/4.0), copyright 2022 AAAS.

have shown promising biocompatibility, providing a wide range of chemically diverse options for biocompatible hydrogels. Synthetic polymers, including polypeptides, poly(vinyl alcohol), poly(acrylic acid), poly(ethylene oxide), derivatives, and copolymers, can be used to fabricate biocompatible hydrogels [57,58,65,66]. The biocompatibility of various hydrogels plays an important role in various bio-related applications such as tissue engineering, biocompatible coatings, bioelectronics, and robotics.

Controlled degradation of hydrogels in physiological environments is also an important property for various bio-related applications. Biodegradation of hydrogels can be induced and controlled by hydrolysis, proteolysis, other enzyme-assisted reactions, and pH/temperature-triggered dissolution reactions [56-58,62,63,65]. Therefore, many biodegradable hydrogels can be easily designed by incorporating proteolytic or hydrolytic functional groups into the polymer network. Although achieving favorable biodegradability and mechanical properties is challenging, the controlled biodegradable properties of hydrogels will provide important functionality for bio-related electronic and robotic applications, which are difficult to achieve using other types of soft materials.

4. Self-healing Properties

Self-healing is the ability of a material to recover its original structure and properties following mechanical or chemical damage. Self-healing hydrogels are particularly important because they provide additional functionalities to restore and recover their structure and functions, ensuring reliable performance with longer

stability (Fig. 3(b)) [37,67-69]. Dynamic covalent bonds and non-covalent interactions can be used to prepare self-healing hydrogels. Specifically, several types of dynamic covalent chemistries, such as imine bonds, boronate-ester complexes, metal coordination, and disulfide exchange, have been widely used to prepare self-healing hydrogels. Self-healing hydrogels can also be fabricated based on a series of non-covalent interactions such as hydrogen bonds, electrostatic interactions, and hydrophobic interactions. In general, dynamic covalent bond-based hydrogels can have stable but slow self-healing speeds owing to slow dynamic equilibria, whereas non-covalent interactions exhibit rapid self-healing speeds with poor mechanical properties. Many self-healing hydrogels have been developed based on diverse natural [70-75] or synthetic [37,76-80] hydrogels.

5. Stimuli-responsiveness

Hydrogels can generate volumetric changes in response to diverse stimuli including temperature, chemicals, light, and electric fields. The large mechanical deformation of hydrogels caused by small changes in the external stimuli makes them promising materials for soft electronic and robotic applications, particularly for developing soft actuators [60,81-84]. Representative stimuli-responsive hydrogels, including temperature responsive hydrogels, chemically-responsive hydrogels, optically-responsive hydrogels, and electrically-responsive hydrogels are described in this section. A detailed description of electrically-responsive hydrogels are provided in Section of Applications of Multi-Functional Conductive Hydrogels.

Temperature responsive hydrogels are among the most extensively studied materials that can swell or shrink depending on the surrounding temperature [85-93]. Volumetric changes are generated depending on the number of hydrophobic and hydrophilic groups in the polymer network of the hydrogels. They are classified into two categories: hydrogels with a lower critical solution temperature (LCST) and hydrogels with an upper critical solution temperature (UCST) [94,95]. Hydrogels with the LCST (e.g., poly(N-isopropy-

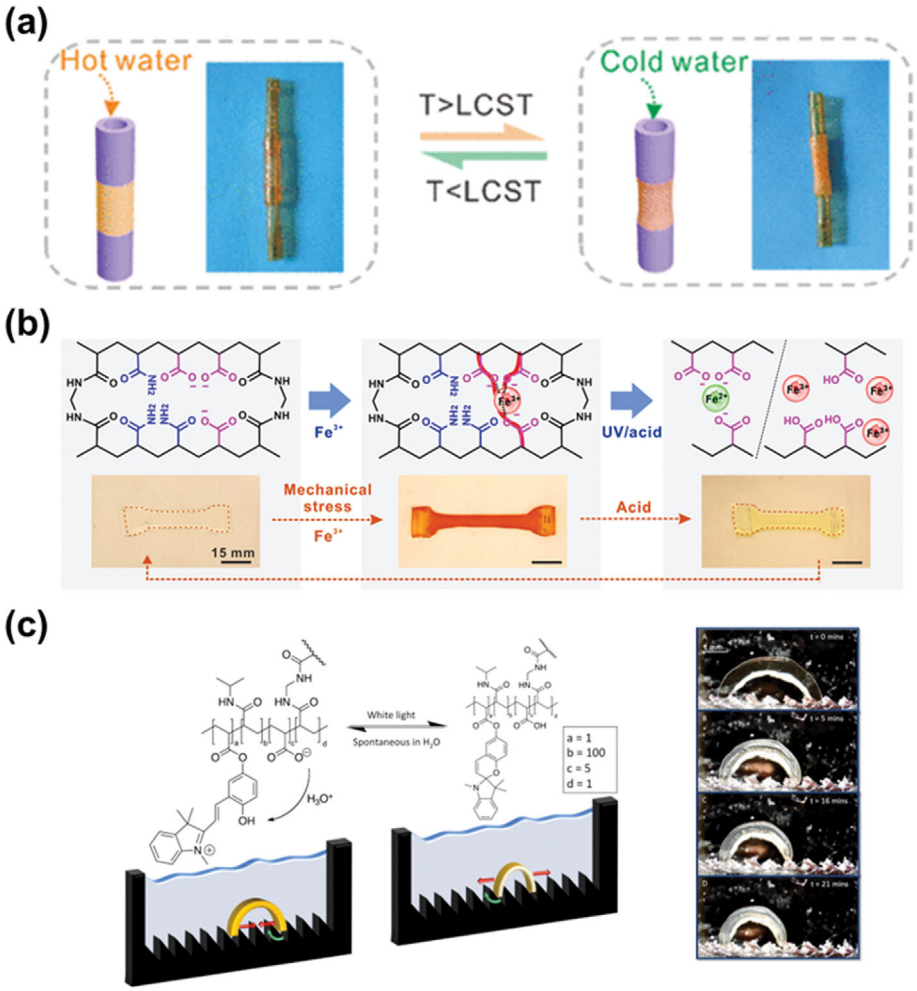

Fig. 4. Unique properties of hydrogel. (a) The asymmetric thermoresponsive hydrogel tubes consisting of thermoresponsive PNIPAAm-PAA and nonresponsive PAM-PAA and its actuation. Adapted from ref. [90] with permission from American Chemical Society, copyright 2019. (b) Poly(acrylamide-co-acrylic acid) hydrogel showing deformation in response of metal ions and acid. Adapted from ref. [103] under the terms of the CC BY-NC, Creative Commons Attribution NonCommercial License 4.0 (https://creativecommons.org/licenses/by-nc/4.0), copyright 2020 AAAS. (c) N-isopropylacrylamide-co-acrylated spiropyran-co-acrylic acid showing optical responsiveness by spiropyran group. Adapted from ref. [115] with permission from Elsevier, copyright 2017.

lacrylamide) (pNIPAM)) exhibit reversible shrinkage above critical temperatures due to decreased solubility in water and swell back to the initial state below critical temperatures (Fig. 4(a)) [85-87,96-98]. By changing the end groups of monomers, the LCST can be modulated. In contrast, hydrogels with the UCST exhibited the opposite behavior at critical temperatures [99-101]. Many studies have been conducted to control the responsivity of hydrogels for various applications.

Chemically-responsive hydrogels showed the most pronounced responsess depending on the specific types of chemical stimuli. In particular, pH provides a facile way to control the mechanical response of hydrogels [102,103]. Depending on the pKa values of the polymeric chain in the hydrogel, the hydrogel can experience ionization of the polymeric chain, which results in expansion of the hydrogel via electrostatic repulsion forces. They can be classified into two types: polyanionic and polycationic chain-based hydrogels. Hydrogels with polyanionic polymer chains experience negative ionization when the pH is higher than the pKa of the polyanionic polymer [104-106]. In contrast, hydrogels with polycationic chains exhibit positive ionization when the pH is lower than the pKa [107]. These expansions can be reversibly de-swollen when the pH reaches their initial states. Based on these working principles, many studies have been conducted to control to the actuatable pH range, response time, and degree of actuation. Other chemical components, including water absorption/evaporation [108,109], organic solvent [110], ions [103], and biomolecules [111,112], can be used to induce volume changes of the hydrogels (Fig. 4(b)).

Optically-responsive hydrogels exhibit a facile control of mechanical deformation under light irradiation. There are several different types of optically-responsive hydrogels depending on their working mechanisms. First, the incorporation of photothermal materials (e.g., AuNPs and carbon-based materials) into thermally-responsive hydrogels can induce mechanical deformation uner light illumination [113,114]. Illuminated light can generate heat in hydrogels through photothermal conversion of the incorporated materials. Secondly, the incorporation of photoswitchable functional groups, such as spiropyran and azobenzene, into the polymeric chains of hydrogels can induce reversible volume changes based on reversible isomerization [115,116]. The dissociation and transformation of spiropyran by UV and visible light, respectively, can induce volume changes in the hydrogel (Fig. 4(c)). In addition, the trans- and cis-transformations of azobenzene by visible and UV light, respectively, can result in swelling and deswelling of the hydrogel.

Electrically-responsive hydrogels provide an effective and accurate way to control the mechanical changes in hydrogels. Electrostatic interactions, electrochemical reactions, and electroosmotic-based mechanisms can be used to electrically actuate hydrogels. The details are described in Section of Applications of Multi-Functional Conductive Hydrogels.

FABRICATION OF HYDROGEL-BASED ELECTRODES

There are four strategies for endowing hydrogels with electrical conductivity. The first strategy involves preparing ionic hydrogels by incorporating ionic salts or liquids dissolved in the aqueous phase of the hydrogel matrix. The second strategy for hydrogel electrode fabrication involves embedding conductive materials (e.g., carbonaceous materials and metal particles) in the hydrogel matrix. Thirdly, water-swellable conductive polymers can provide electrical pathways and construct a hydrogel matrix. Another strategy is to form conductive layers on the hydrogel surfaces. The recent advances and challenges in hydrogel fabrication are described in this section and summarized in Table 1.

1. Ion-conductive Hydrogel

Ionically conductive hydrogels (IC hydrogels) are prepared by dissolving mobile ions (e.g., electrolytes, polyelectrolytes, and ionic liquids) in the water phase of a hydrogel, similar to biological tissues containing liquid electrolytes (Fig. 5(a)) [26,35,37,48,117-120]. Because of the nano/micro-scale porous structures in hydrogels, the free diffusion of mobile ions in the polymer network of the hydrogel enables the transport of electrical charges through the hydrogels. In addition, various unique properties can be combined with IC hydrogels because of their facile preparation methods, allowing their application in various functional hydrogels. Keplinger et al., reported stretchable and transparent ionic conductors based on polyacrylamide hydrogels, which have attracted significant research attention. The reported IC hydrogels exhibit high ionic conductivity, favorable mechanical properties (stretchability >1,000%, modulus <100 kPa), and transparency. IC hydrogels have made significnat progress by introducing diverse mechanical properties [35,37,48, 120] and functionalities [118,119,121].

However, IC hydrogels suffer from intrinsically limited electrical conductivity, slow response times, undesirable electrochemical reactions under physiological conditions, and deteriorating performance due to the release of incorporated ions. It is necessary to develop approaches to obtain higher operational stability in physiological environments for a wide range of applications. For example, Zhao et al. reported IC hydrogels with enhanced physiological stability based on poly(ethylene glycol)/salt phase-separated hydrogels, which prevented the diffusion of liquid electrolytes into the surroundings (Fig. 5(b)) [118]. In addition, the introduction of elastomer coated-IC hydrogels provided effective ways to prevent the release of liquid salts as well as additional functionalities.

2. Conductive Polymer-based Hydrogels

In contrast to typical electrically insulating polymers, conjugated polymers can possess electrical conductivity. Specifically, the delocalization of electrons through conjugation in the backbones of polymers composed of alternating single and double bonds allows the conduction of electrons through polymeric chains. A single network or an interpenetrating network of water-swellable conductive polymer hydrogels (CP hydrogels) (e.g., polypyrrole (PPy), polyaniline (PAni), and poly(3,4-ethylene-dioxythiophene) (PEDOT)) can be used to fabricate conductive hydrogels [70,72,77,122-130]. It is particularly noteworthy that electrical conductivity at the molecular level (i.e., polymeric chain) permits additional flexibility as well as ionic conductivity, creating nanometer (or sub-nanometer) scale molecular-level electric double layers (EDL) through polymeric networks in hydrogels. Ionic and electronic conductivities in molecular-level are promising for various bio-related applications.

Lu et al. reported a pure PEDOT:PSS hydrogel composed of interconnected PEDOT:PSS nanofibrils based on dimethyl sulfox-

Table 1. Electrical conductivities and other properties of hydrogel electrodes

Type	Materials	Conductivity (S cm^{-1})	Other properties	Ref.
IC hydrogel	PAAm (LiCl)	10^{-3}~0.5	- Modulus ~ 100 kPa - Stretchability >1,000% - Transparency ~ 98.9%	[35]
	Trehalose-modified PAAm	0.0032	- Modulus ~ 365 kPa - Stretchability ~ 2,520% - Toughness ~ 5,116 J m^{-2} - Self-healing (5s)	[37]
	Bentonite incorporated cellulosic hydrogel	0.089	- Modulus ~ 3.56 MPa - Stretchability ~ 50% - Toughness ~ 0.45 MJ m^{-3} - Freezing tolerant	[120]
	PAAm (LiCl)	0.01	- Modulus ~ 12 kPa - Stretchability ~ 1,000% - Transparency ~ 98%	[121]
CP hydrogel	PEDOT:PSS	40	- Modulus ~ 2 MPa - Stretchability ~ 35% - Physiological stability (3 months) - Electrochemical stability	[126]
	PEDOT:PSS/PU biphase	>11	- Modulus <1 MPa - Stretchability >400% - Toughness 3,300 J m^{-2} - Mech./elect. stability (10,000 cyc) - 3D printing	[130]
	PAA-templated PEDOT:PSS	247	- Modulus ~ 25 kPa - Stretchability ~ 610% - Toughness 1 MJ m^{-3}	[129]
CN hydrogel	LM/CNT embedded PAAm hydrogel	0.94	- Stretchability ~ 2,200% - Transparency ~ 93% - Self-healing	[134]
	Ag flakes embedded PAAm-alginate hydrogel	374	- Modulus <10 kPa - Stretchability ~ 250%	[133]
	Ag flakes/LM embedded PVA-Borax gel	700	- Modulus ~ 20 kPa - Stretchability >400% - Self-healing - Anti-drying	[80]
CC hydrogel	LM-printed P(AAm-co-MAAc)	2,000	- Stretchability ~ 630% - Self-shaping	[141]
	Carbon electrode-coated Nafion	780	- Modulus ~ 1,330 MPa - Stretchability ~ 20% - Electrochemical activity	[150]
	Pt-reduced Nafion	4,000	- Modulus ~ 150 MPa - Electrochemical activity	[145]
	Au cluster-assembled PAA-co-PAN hydrogel	1,000	- Modulus ~ 0.35 MPa - Stretchability <5% - Electrochemical activity	[148]
	Au NPs assembly on PAA-based hydrogels	4,310	- Modulus ~ 4 MPa - Stretchability ~ 20% - Electroosmosis	[178]
	Au NPs assembly on PAA-based hydrogels	41,000	- Modulus ~ 4.2 MPa - Stretchability ~ 110% - Electroosmosis	[179]

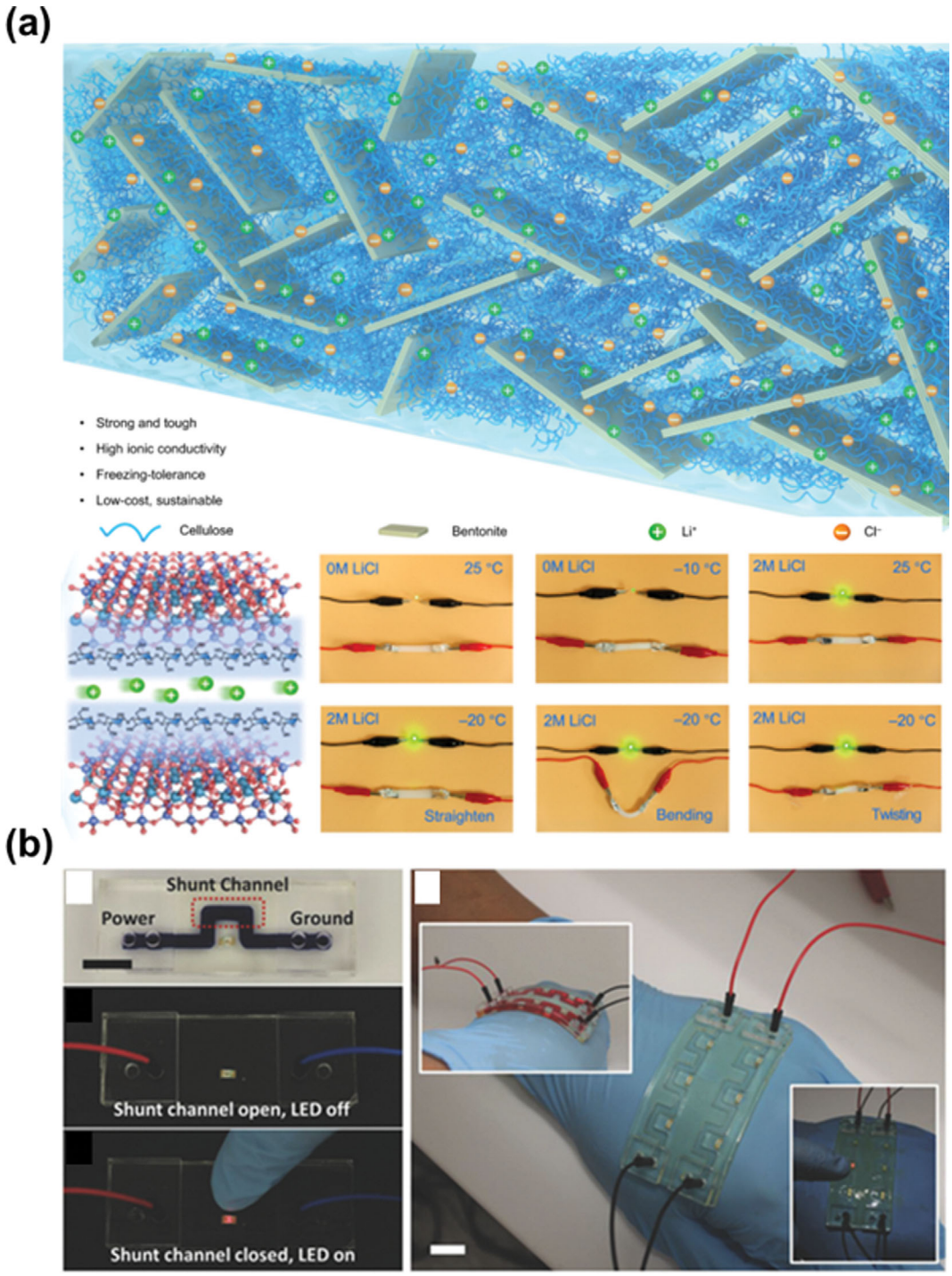

Fig. 5. Ion-conductive hydrogel. (a) Bentonite incorporated cellulose hydrogel showing high ionic conductivity and mechanical properties. Adapted from ref. [120] under the terms of the CC-BY Creative Commons Attribution 4.0 International License (https://creativecommons.org/licenses/by/4.0), copyright 2022 Springer Nature. (b) Hydrogel ionic circuits based on salt/poly(ethylene glycol) aqueous two-phase systems showing improved operation stability. Adapted from ref. [118] with permission from John Wiley and Sons, copyright 2018.

ide-added hydrogel solution preparation and subsequent dry-annealing (Fig. 6(a)) [126]. The optimized dry-anneal process (i.e., amount of DMSO and anneal conditions) led to an electrical conductivity of 20 S cm^{-1} with stretchability of over 35%. Although hydrogels with a single network of conductive polymers can achieve relatively high electrical conductivity, they typically exhibit limited mechanical properties.

Mechanically robust CP hydrogels can be prepared by forming interpenetrating networks of conductive polymers within tough hydrogel matrices. However, this approach typically led to low elec-

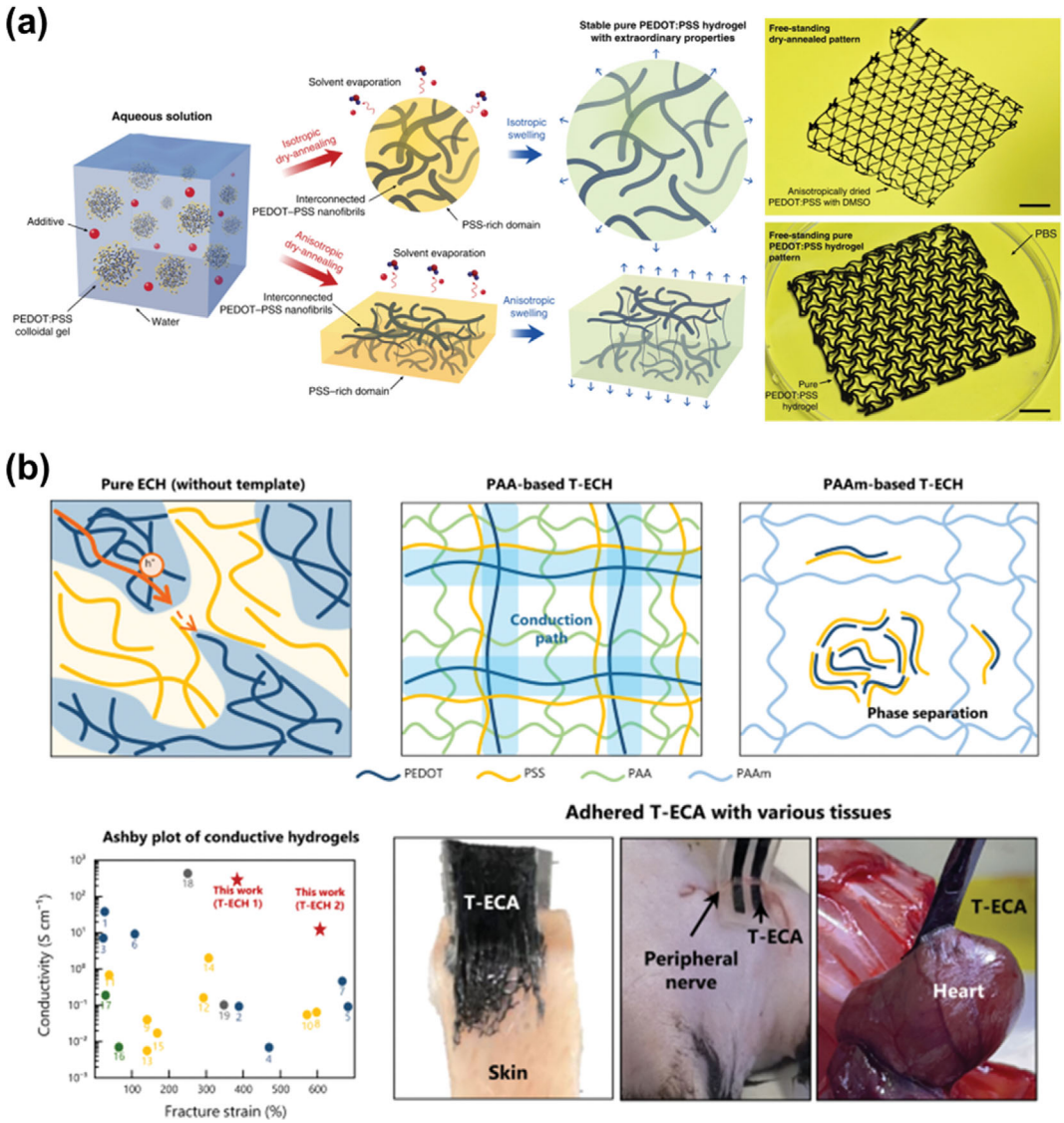

Fig. 6. Conductive polymer-based hydrogel. (a) Pure PEDOT:PSS hydrogels composed of interconnected networks of PEDOT:PSS nanofibrils and patterned images. Adapted from ref. [126] under the terms of the CC-BY Creative Commons Attribution 4.0 International License (https://creativecommons.org/licenses/by/4.0), copyright 2019 Springer Nature. (b) PEDOT:PSS electrically conductive hydrogel fabricated poly(acrylic acid) template-directed assembly method, showing high conductivity and good adhesion to various tissues. Adapted from ref. [129] under the terms of the CC-BY Creative Commons Attribution 4.0 International License (https://creativecommons.org/licenses/by/4.0), copyright 2023 Springer Nature.

trical conductivity (<0.3 Scm^{-1}) due to limited degree of electrical connectivity in hydrogel matrix [33]. In addition, attempts to increase the amount of conductive polymers in hydrogels result in mechanically weak structures, showing challenging problems of trade-off between electrical and mechanical properties.

Chong et al. introduced a template-directed assembly method to fabricate hydrogels with high electrical conductivity and robust mechanical properties (Fig. 6(b)) [129]. Polyacrylic acid (PAA) was used as a template material to suppress bulk aggregation of PEDOT chains, resulting in nanoscale fiber networks of PEDOT. The resultant electrically conductive hydrogel formed by template-directed assembly method (T-ECH) showed a significantly enhanced electrical conductivity (247 S cm^{-1}) with tissue-like softness (modulus ~25 kPa), high stretchability (610%), and toughness (1 MJ m^{-3}). In addition, Zhou et al. reported a two-phase hydrogel containing a bi-continuous conducting polymer inside a hydrogel matrix (BC-CPH) that could address the challenges related to conflicts between electrical and mechanical properties [130]. BC-CPH comprised of an electrical phase (PEDOT:PSS) and a mechanical phase (hydrophilic polyurethane) to achieve favorable electrical and mechanical properties, simultaneously. The prepared BC-CPH exhibited high electrical conductivity (>11 S cm^{-1}) and stretchability (>400%), fracture toughness (>3,300 Jm^{-2}) and compliance (Young's modulus below 1 MPa). However, it is still challenging to impart high electrical conductivity and many functionalities to hydrogels, as described in Section of Unique Properties of Hydrogels.

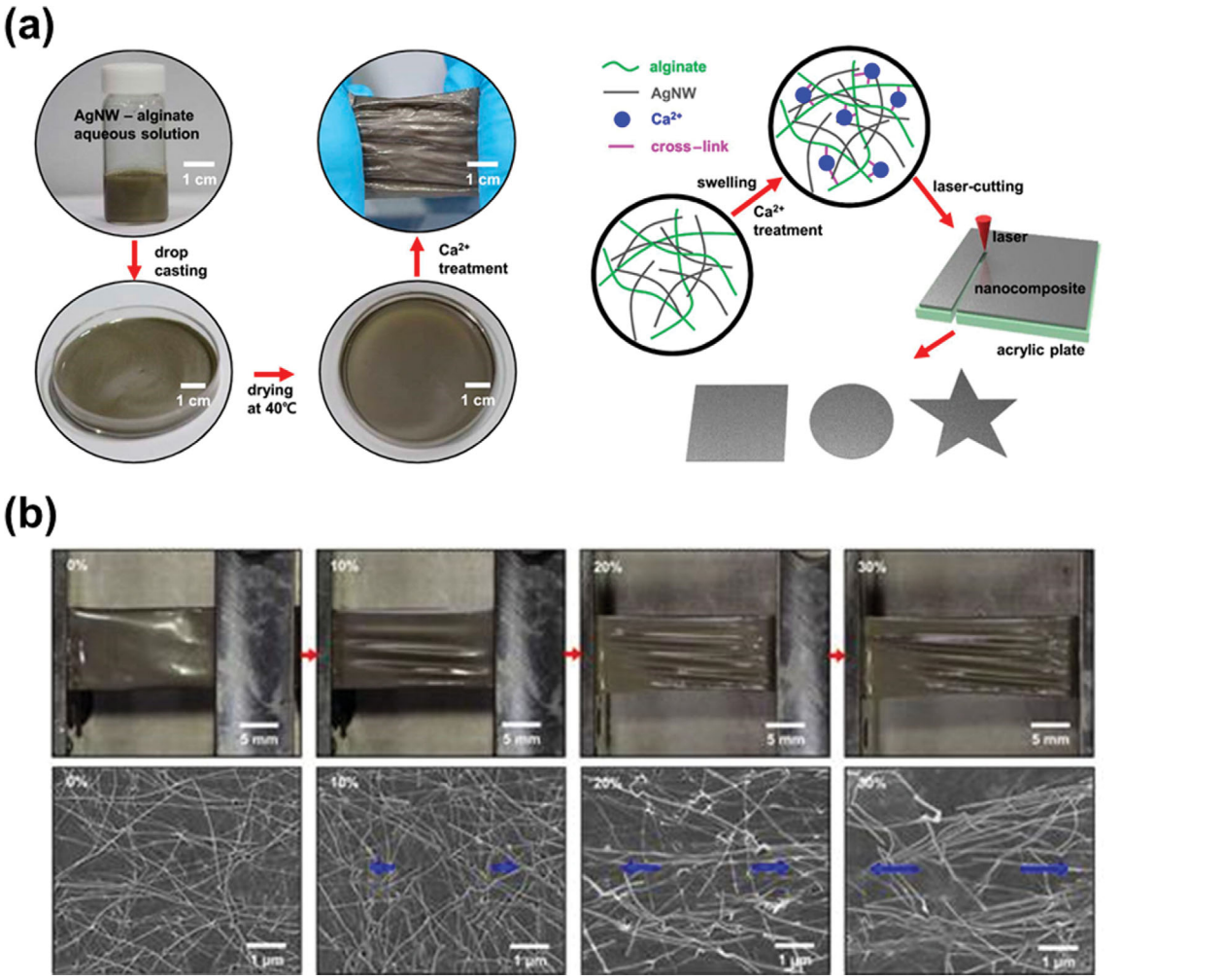

Fig. 7. Conductive nanocomposite hydrogel. (a) Fabrication procedure for preparing AgNWs embedded PAAm hydrogel. (b) Photographic and SEM images of prepared PAAm-AgNWs hydrogel at stretched state showing interconnected structures. Adapted from ref. [131] under a Creative Commons Attribution (CCBY) license (http://creativecommons.org/licenses/by/4.0), copyright 2018 AIP Publishing.

3. Conductive Nanocomposite Hydrogels

Preparation of hydrogel composites prepared by incorporating conductive components into hydrogel matrices are widely used to prepare conductive hydrogels. The conductive components embedded in the hydrogel matrices provide pathways for electrical currents. For this purpose, metallic components (e.g., nanowires, plates, micro/nanoparticles of Pt, Ag, Au, and EGain) [80,131-134] and carbonaceous conductive materials (e.g., carbon nanotubes, graphene, and MXene) [78,134-139] have been used (Fig. 7). Compared with conductive elastomers prepared by incorporating microparticles of liquid metal (e.g., eutectic gallium indium) and silver, which show a high degree of stiffness, conductive nanocomposite hydrogel (CN hydrogels) can have favorable tissue-like softness along with additional functionalities.

CN hydrogels have shown the potential to develop conductive hydrogels that can simultaneously satisfy high electrical conductivities and tissue-like softness at the same time. However, previous studies have encountered a trade-off between simultaneously achieving high electrical conductivity and mechanical softness in CN hydrogels. To obtain higher electrical conductivity, larger amounts of metallic materials are desired; however, metallic materials are susceptible to aggregation inside the hydrophilic hydrogel matrix, resulting in undesirable mechanical and electrical properties of CN hydrogels. The use of carbonaceous materials has faced similar problems. The hydrophobic nature of carbonaceous materials leads to self-aggregation inside the hydrogel matrix, preventing the generation of percolated electrical pathways. In addition, several cytotoxic materials, such as CNT, can be exposed to the external environment, resulting in undesirable effects on biological tissues [140]. Recently, CN hydrogels based on noble metals have shown promising results, achieving higher electrical conductivities with better controllable mechanical properties as shown in Table 1.

Ohm et al., reported silver-polyacrylamide-alginate hydrogel composite having high electrical conductivity (374 Scm^{-1}), tissue-like softness (a low Young's modulus (<10 kPa) as low as soft biomaterials), and high stretchability (250% strain) at the same time [133]. These high-performance CN hydrogels were prepared based on the controlled assembly of Ag microflakes in a hydrogel matrix (PAAm-alginate hydrogel), which generated percolated electrical pathways. This was attributed to a partial dehydration process, which induced

effective percolation pathways for the electrical current with a small amount of silver micro-flakes (<10 vol%). Specifically, the prepared CN hydrogels (Ag content of 5 vol%) showed dramatically decreased resistance from the order of kiloohms (conductivity ~0.13 Scm^{-1}) to 1.14 Ω (conductivity ~374 Scm^{-1}) by dehydration process (90 min). Highly conductive CN hydrogels with favorable tissue-like mechanical properties have demonstrated promising applications in electronic and robotic devices.

The incorporation of conductive metallic materials, along with a partial dehydration method that can be easily applied to a variety of hydrogels, has also been applied to self-healing hydrogels. Zhao et al. reported a self-healing, electrically conductive hydrogel composite employing a self-healing hydrogel (poly(vinyl alcohol)-sodium borate, PVA-Borax) [80]. The hydrogel composite was fabricated by embedding Ag microflakes and liquid metal microdroplets in PVA-Borax gel matrix. The addition of liquid metal micodroplets and dry annealing permit the generation of effective percolating electrical pathways with low amounts of metallic components. The prepared composite exhibited high electrical conductivity without compromising the favorable mechanical properties

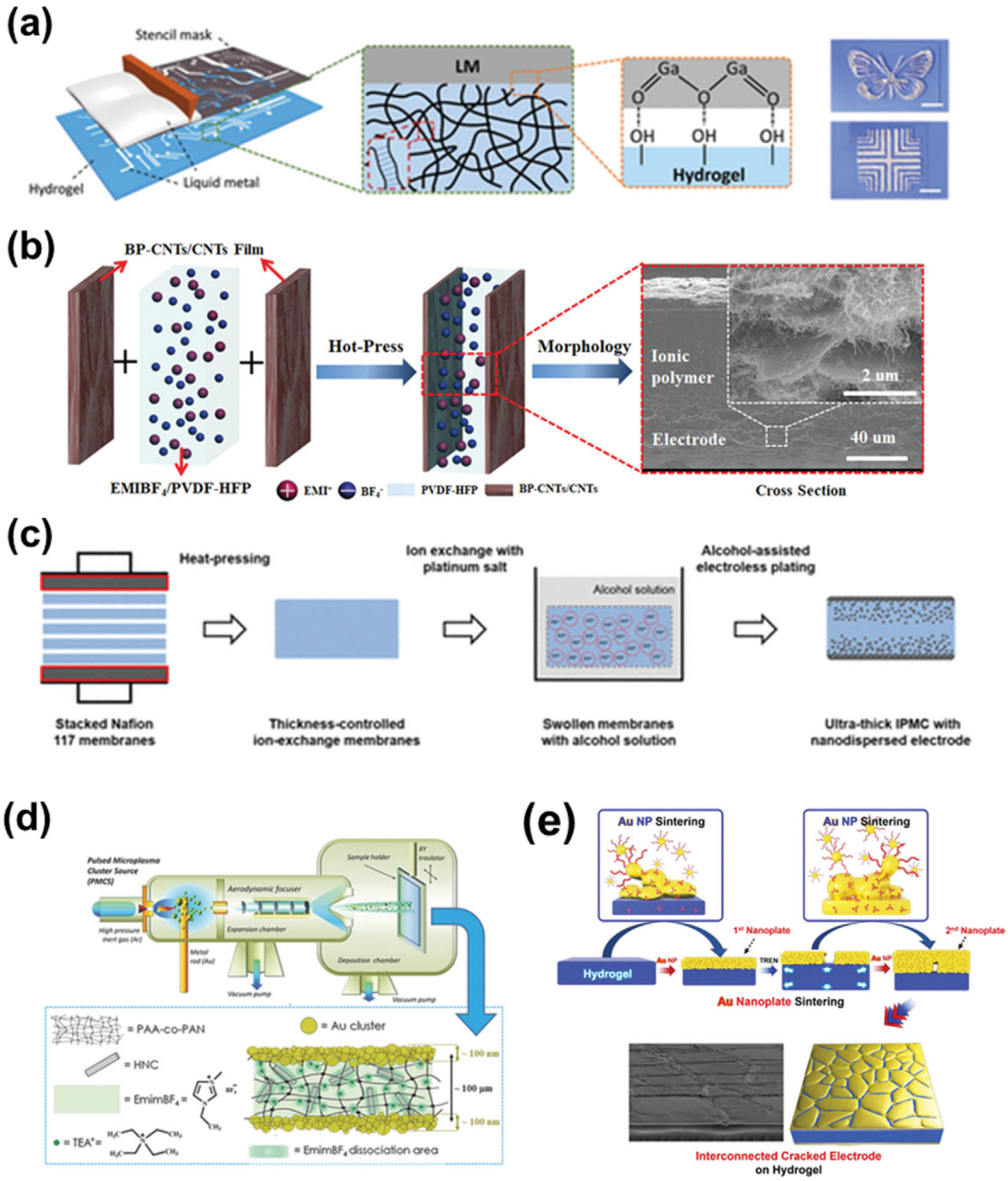

Fig. 8. Conductive layer-coated hydrogel. Schematic illustration of various coating methods for preparing conductive hydrogels: (a) printing, (b) transfer, (c) chemical reduction, (d) supersonic cluster beam implantation, and (e) LbL-assembly. Adapted from ref. [141] with permission from John Wiley and Sons, copyright 2021, from ref. [143] with permission from John Wiley and Sons, copyright 2018, from ref. [145] with permission from American Chemical Society, copyright 2017, from ref. [148] with permission from John Wiley and Sons, copyright 2016, and from ref. [178] with permission from American Chemical Society, copyright 2020, respectively.

of PVA-Borax gel (low stiffness (elastic modulus of ~20 kPa), a high strain limit (maximum strain >400%), and self-healing). Specifically, the resultant CN hydrogels exhibited a high electrical conductivity of 7×10^2 Scm^{-1} along with a low Young's modulus (~20 kPa), high stretchability (>400% strain), and effective self-healing properties. Moreover, the addition of ethylene glycol instead of water to the hydrogels enabled stable operation under ambient conditions for over 24 h, demonstrating their anti-drying properties. Despite recent promising results for CN hydrogels, their reported electrical conductivity is still lower than that of nanocomposite soft electrodes based on elastomers [12-17].

4. Conductive Coating on Hydrogels

In contrast to other approaches offering limited electrical conductivity originating from a poor density of conductive materials, the conformal deposition of densified conductive materials on hydrogel surfaces allows for endowing hydrogel with a high degree of electrical conductivity. Previously reported approaches for forming conductive layers on soft substrates (polymer or elastomer substrates) can be applied; however it is difficult considering unique features of hydrogels. Different methods, including printing, transfer, cluster beam implantation, chemical reduction, and nanoparticle assembly, can be used to form electrode layers on hydrogel surfaces. However, forming mechanically stable and high-performance electrode layers on hydrogels is challenging because of the substantial hydrated layers on the hydrogel surface.

4-1. Printing

Hao et al. reported tough liquid-metal-printed hydrogels with superior electrical conductivity as shown in Fig. 8(a). A liquid metal alloy (LM, eutectic gallium-indium) doped with Ni particles was patterned on the surface of poly(acrylamide-co-methacrylic acid (P(AAm-co-MAAc)) hydrogels using the stencil-printing method [141]. They achieved robust interfacial bonding between the liquid metal layer and the hydrogel via hydrogen bonding. Therefore, the resultant hydrogel electrode showed unprecedentedly high electrical conductivity (2,000 S cm^{-1}), stretchability (630%) and low Young's modulus, which have been difficult to be realized by previous studies. However, the LM residue readily formed by the mechanical rubbing of LM in the liquid state remains problematics, particularly for bioelectric applications.

Hao et al. introduced a biopolymer-based hydrogel (gelatin-alginate hydrogel) for the patterned printing of LM [75]. The prepared hydrogels exhibit various favorable properties and functionalities for electronic devices, including transparency, self-healing, self-adhesion, mechanical robustness, and biodegradability. In particular, biodegradable functionalities (degradation within 10 h in a gelatin hydrolase solution) will play an important role in the development of transient biomedical applications. The LM alloy (EGaIn) with added Fe particles was used for good printability of the gelatin-alginate hydrogel. Various LM shapes can be coated onto hydrogels by stencil printing.

4-2. Transfer

The transfer of individually prepared electrodes onto elastomer surfaces is widely used to prepare soft electrodes for various soft electronic applications. However, the intrinsic nature of the hydrogel, which has a high water content and a significant hydrated surface layer, poses significant challenges in forming robust bonding antagonistic materials, such as metallic or carbonaceous layers with a high modulus. Therefore, hydrogels coated with electrode layers have typically been susceptible to delamination of electrode layers under large mechanical deformation. To obtain robust interfacial bonding between the electrode layer and hydrogel, transfer by heat pressing methods is necessary. Several different types of carbonaceous materials, such as CNT, graphene, and MXene, can be transferred onto hydrogel surfaces using heat pressing methods. Carbon composites with electrical conductivity and electrochemical activity formed by polymers, which can assist in forming bonds with the hydrogel, were used and transferred using the heat pressing method (Fig. 8(b)) [142,143].

However, hydrogel electrodes fabricated using the aforementioned transfer method typically exhibit stiff mechanical properties. Li et al. introduced a soft-interlayer between the electrode layer and the hydrogel to realize a hydrogel electrode with tissue-level softness [144]. Specifically, polystyrene-ethylene-butylene-styrene (SEBS H1052) was used as an interlayer because of its Young's modulus intermediate between that of the electronic materials and hydrogels, as well as its robust bonding capability with both layers. When 1.2 μm-thick SEBS interlayer was introduced on a polyacrylamide (PAAm) hydrogel (200 μm-thick), the resultant interlayer-hydrogel substrates showed tissue-like softness (almost no effects on modulus of hydrogel) with high stretchability, which was difficult to achieve with conventional soft electrodes based on PDMS and SEBS. Based on a thin soft interlayer design, stretchable electronic devices based on hydrogel substrates have been demonstrated, showing an effective Young's modulus as low as 5.2 kPa.

4-3. Chemical Reduction

Electroless plating, based on the chemical reduction of metal ions, enables the deposition of metal layers on the surface of a polymer [145-147]. Additionally, ionomers (or hydrogels) containing metal salt solution in their matrices can be used as substrates for electroless plating. After immersing the metal salt solution in the ionomer, a chemical reducing agent was added to reduce the metal ions absorbed on the surface of the ionomer, resulting in the deposition of a metal layer on the surface. Depending on the concentration of the metal ions, reaction temperature, and reaction time, the degree of metal layer deposition can be controlled. Nafion membranes are widely used for this purpose. Metal-ion adsorption and chemical reduction were conducted to achieve electrode layers with high electrical conductivity (~4,000 S cm^{-1}) (Fig. 8(c)) [145]. However, hydrogel electrodes prepared via chemical reduction typically exhibit substantially stiff mechanical properties because of the thick electrode layers on the hydrogel surface.

4-4. Supersonic Cluster Beam Implantation

As previously described, the formation of highly conductive thin electrode layers on a hydrogel surface remains challenging. The supersonic cluster beam implantation (SCBI) method was suggested to deposit thin Au cluster assembled electrodes (~100 nm thick) on the hydrogel surface with almost no effect on the mechanical properties of the hydrogels (Fig. 8(d)) [148]. In contrast to sputtering and thermal evaporation which require a high-vacuum state and are difficult to apply into hydrogels, SCBI allows the growth of a metallic layer on the surface by the supersonic implantation of gold nanoparticles. Specifically, a highly collimated beam of neu-

tral metal clusters was directed onto a hydrogel (poly acrylic acid-poly acrylamide copolymerized hydrogel). The implanted clusters gradually grew on the hydrogel surface without any thermal or chemical damage. As the process goes on, the thickness of deposited electrode layers grows from 6 nm to 100 nm, decreasing electric resistance from $6\times10^5\ \Omega\ cm^{-2}$ to $95\ \Omega\ cm^{-2}$.

4-5. Assembly of Conductive Materials

Conductive materials in solution can also be used to prepare the electrode layer by inducing the assembly of nanomaterials on the hydrogel surface. Drop-casting of the solution, followed by thermal drying, has been readily used to deposit various types of carbonaceous conductive materials (e.g., MXene and graphene). For example, Umrao et al. formed electrode layers on a Nafion surface using a MXene dispersed solution [149]. First, a $Ti_3C_2T_x$ MXene suspension was mixed with PEDOT:PSS in N,N′-dimethylformamide. Then, the solutions were dropped on surface of Nafion-ionic liquid infiltrated membrane, followed by dried at 90 °C for 40 minutes. The ionic crosslinking of MXene and PEDOT:PSS enables the formation of robust bonds on the Nafion surface. Graphene-based electrodes can be prepared on Nafion surfaces in a similar manner. The solution mixture of graphitic carbon nitride and nitrogen-doped graphene was dropwise deposited on one surface of Nafion-IL membrane, and then dried at 80 °C [150]. However, without consideration on interfacial adhesion, simple drop casting along with thermal drying cannot avoid insufficient adhesion between electrode layer and hydrogel surface. Such weak adhesion results in the flaking or delamination of the electrode layer from the hydrogel surface, restricting its wide application.

In addition to drop-casting methods, which suffer from poor mechanical properties originating from interfacial interactions, a layer-by-layer (LbL) assembly can be used to form highly conductive, compliant, and robust electrode layers on hydrogel surfaces [151-162]. Based on the complementary interactions between different materials, LbL assembly can provide versatile methods to form various types of composites composed of organic, inorganic, and organic-inorganic hybrid materials [163-172]. Therefore, a variety of nanocomposites with desirable electronic, optical, electrochemical, and biological features can be prepared on various types and shapes of soft substrates with controlled film thickness, composition, functionality. In particular, a small molecule linker-based LbL assembly has been suggested to form high-performance electrodes for energy harvesting, energy conversion, and energy storage devices based on the minimized interfacial resistance between neighboring nanomaterials [172-177].

Previous LbL assembly has been effective for application on dry substrates. Despite significant advances in LbL assembly for the preparation of high-performance soft electrodes, it is still challenging to apply LbL assembly principles to hydrogels because of the large water content and significantly hydrated layers on the surfaces. Recently, Ko et al., reported a hydrophilic/hydrophobic LbL assembly method that was modified for the application to hydrogel surfaces [178,179]. Specifically, tetraoctylammonium bromide (TOABr)-Au NPs dispersed in toluene were sequentially LbL-assembled with amine-functionalized linkers (tris(2-aminoethyl) amine or poly(ethyleneimine)) dispersed in DI water based on complementary covalent-bonding interactions. It is important to note that during the ligand exchange reactions between bulky TOABr ligands, loosely bound Au NPs and amine-functionalized molecules, assembly as well as room-temperature sintering of Au NPs were observed. While the previously reported interfacial assembly of nanoparticles induces fragile monolayer sheets whose nanoparticles are separated by long ligands, our approach features partial sintering, resulting in the continuous growth of Au NPs nanoplate to overall surfaces of the hydrogels, as shown in Fig. 8(e). Therefore, continuous growth of sintered Au NPs in the lateral and vertical dimensions can be observed at the hydrogel surface. Moreover, the incorporation of amine-functionalized linkers in Au NPs nanoplates enabled to form strong adhesion of Au NPs-assembled electrode layers with hydrogel surface, which was difficult achieve with other types of coating methods. Based on this process, highly conductive, mechanically compliant, and robust metallic layers can be formed on the surfaces of arbitrary shapes and types of hydrogels, which are difficult to achieve using conventional coating methods. Notably, an additional deswelling process can generate wrinkled electrode structures, which are highly beneficial for the electrical and mechanical properties of the electrodes. The resulting electrodes exhibited substantially high electrical conductivity of ~41,000 S cm^{-1}, which is a few orders of magnitude higher than that of previously reported hydrogel electrodes. In addition, high conductivity can be maintained up to stretching of 100%, overcoming the trade-off problems of previously reported hydrogel-based electrode fabrication methods. This approach demonstrates promising potential for the development of multi-functional hydrogel electrodes with high electrical conductivity and the desired mechanical properties, based on LbL assembly methods.

APPLICATIONS OF MULTI-FUNCTIONAL CONDUCTIVE HYDROGELS

1. Hydrogel-based Electronics

1-1. Electronics Based on Ionic Hydrogels

Ionic hydrogels that contain mobile ions as charge carriers play a key role in the development of new types of ionotronic devices. Kim et al. reported a soft and transparent touch panel based on a PAAm hydrogel with LiCl salts (2 M) dissolved in water phase in hydrogel [121]. Hydrogel-based touch panels can be operated using surface-capacitive methods. A uniform electrostatic field was generated across the hydrogel by applying the same voltage through all corners of the ionic hydrogel. When a human finger, which is conductive, touches the ionic hydrogel surface, a potential difference is created between the electrode positioned at the corner of the hydrogel and the touch point, by flowing current through the touched conductor (finger). Based on the amount of the current flowing through the touched conductor, the distance between the electrodes can be determined, providing information regarding touched position. The ionic touch panel could be operated even when stretched by over 1,000% by taking advantages of the superior mechanical properties of the hydrogels. Moreover, a series of promising applications such as drawing figures, playing music, and game can be demonstrated.

In addition to the use of ionic hydrogel as sensors, the integration of ionic hydrogels with dielectric elastomers can impart unique

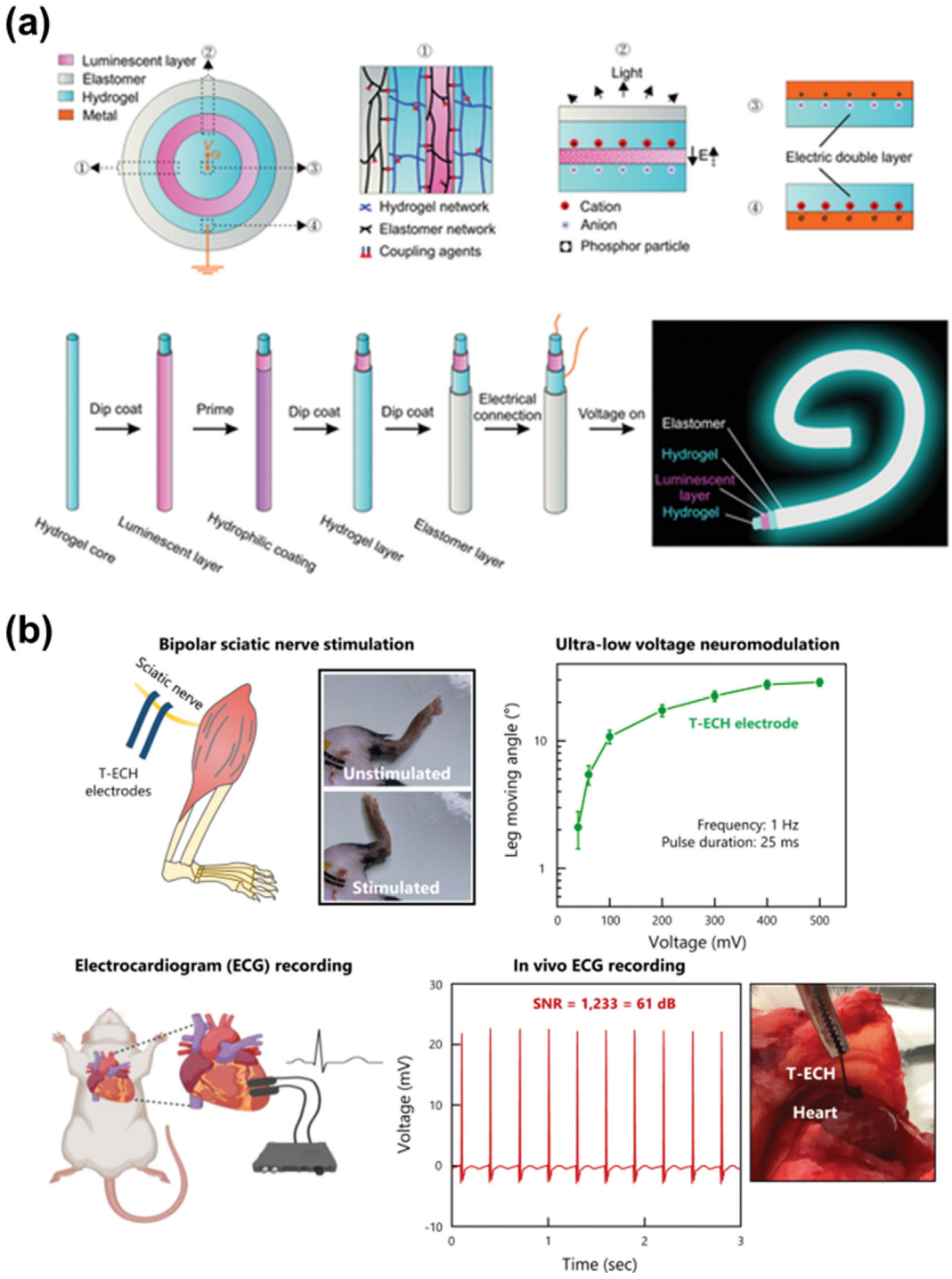

Fig. 9. Electronic applications based on IC and CP hydrogels. (a) Fabrication procedure for ionotronic luminescent fiber composed of LiCl dispersed PAAm hydrogel core and ZnS:Cu particles dispersed PDMS layer and its light illumination image. Adapted from ref. [180] with permission from John Wiley and Sons, copyright 2021. (b) Nerve stimulation and electrocardiogram recording of T-ECH hydrogel. Adapted from ref. [129] under the terms of the CC-BY Creative Commons Attribution 4.0 International License (https://creativecommons.org/licenses/by/4.0), copyright 2023 Springer Nature.

functionalities to ionotronic devices. Lee et al. reported highly transparent (99.6%) and stretchable (330%) triboelectric nanogenerators fabricated by integrating a PAAm hydrogel with LiCl and PDMS [50]. The prepared ionotronic devices can function as triboelectric nanogenerators based on induced electrostatics and contacted electrification. Based on this triboelectric working principle, a self-cleanable, stretchable, and transparent touch panel device was fabricated with a maximum output power density of 4.22 W m^{-2}. Yang et al. reported an ionotronic luminescent device based on coaxial fiber structures consisting of a LiCl dispersed PAAm

hydrogel core and a ZnS:Cu particle dispersed PDMS layer, as shown in Fig. 9(a) [180]. Applying an electric field (3 V μm^{-1} at 1 kHz) through the ionic hydrogel, the fiber can emit the light, demonstrating broad application of hydrogel ionotronics with different architectures.

Despite research efforts, it remains difficult to develop ionic hydrogels that can effectively control ionic migration in the replication information process in biological systems. Tian et al., reported an ionic hydrogel whose ionic conductivity could be modulated by optical means to emulate biological synaptic function [181]. Specifically, the use of supramolecular clumps in hydrogels enables control of the release of mobile ions by optical stimuli. Based on the dynamic assembly assisted optical control of ionic conductivity, the prepared hydrogel device could perform an information processing function that emulates the synaptic functions.

1-2. Electronics Based on Conductive Polymer-based Hydrogels

The T-ECH (described in Section of Fabrication of Hydrogel-Based Electrodes) demonstrated promising bioelectronic applications owing to its high electrical conductivity and multiple functionalities (biocompatibility, tissue-like softness, toughness, and strong adhesiveness), as shown in Fig. 9(b) [129]. In particular, the T-ECH robustly bonded to the tissue enabled efficient nerve stimulation and record of electrophysiological signals. Specifically, an extremely low simulating voltage (40 mV at 1 Hz) evoking leg movements was achieved based on superior electrical properties (high electrical conductivity and large surface area of electrochemical reactions), as well as robust electrical interfaces with biological tissues. Moreover, when the T-ECH was applied to the beating heart,

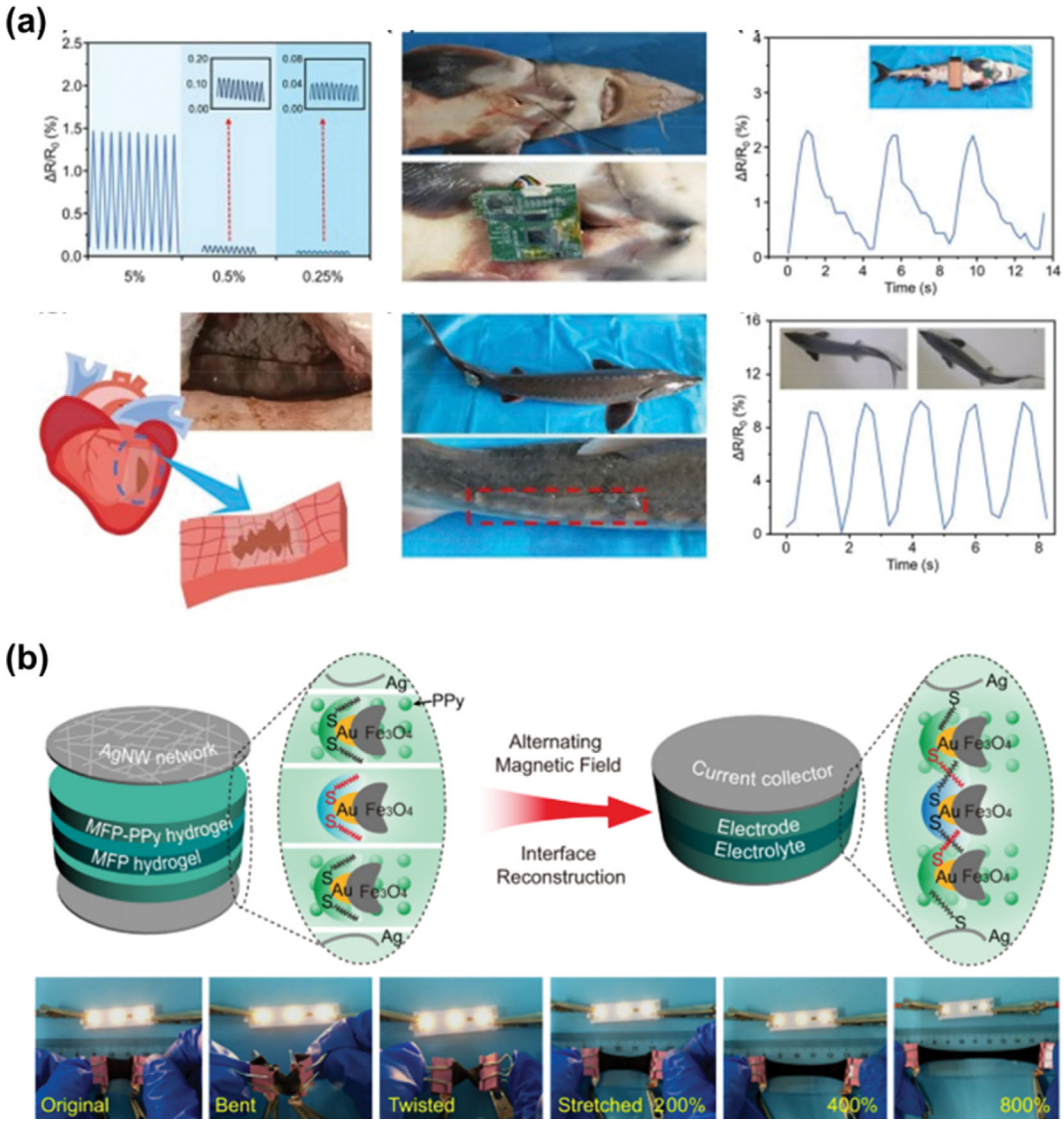

Fig. 10. Electronic applications based on CN and CC hydrogels. (a) Wireless sensing of tail movement and heart beating of the Chinese sturgeon based on polyacrylamide incorporated with CNT bridged LM (eutectic gallium-indium). Adapted from ref. [134] with permission from Elsevier, copyright 2023. (b) Schematic illustration of the supercapacitor fabricated by sandwiching two MFP-PPy hydrogel coated with AgNW film layers. Adapted from ref. [79] under the terms of the CC-BY Creative Commons Attribution 4.0 International License (https://creativecommons.org/licenses/by/4.0), copyright 2023 Springer Nature.

it exhibited a substantially high SNR, enabling high-quality electrophysiological signals recording compared to those of other types of ECG devices.

Bi-continuous conducting polymer hydrogel (BC-CPH) based on PEDOT:PSS (described in Section of Fabrication of Hydrogel-Based Electrodes) demonstrated all-hydrogel bioelectronic devices based on its high electrical conductivity (>11 S cm^{-1}), and desirable mechanical properties (stretchability >400%) and toughness (>3,300 J m^{-2}). The prepared BC-CPH could be successfully applied to bioelectric interfaces that efficiently show electrophysiological recording and stimulation performance. Moreover, long-term electrophysiological efficacy was also demonstrated, originating from the robust interfaces and biocompatibility [130].

1-3. Electronics Based on Conductive Nanocomposite Hydrogels

In contrast to conductive polymer-based hydrogel electrodes, which have a limited chemical composition, embedding conductive components can yield a wide range of polymer matrices and electrical components. This intrinsic feature of the fabrication method enables diverse functionalities and higher electrical conductivity. Recently reported hydrogel electrodes fabricated by embedding silver flakes (described in Section of Fabrication of Hydrogel-Based Electrodes) exhibited higher conductivity along with tissue-like softness (~20 kPa) and several functionalities (self-healing and biodegradation) [80,133]. Using this CN hydrogel, self-healable circuit connectors for soft robots and electromyography (EMG) sensing electrodes have been demonstrated, showing superior electrical and mechanical performances of the hydrogel electrodes.

Sun et al. reported CN hydrogel-based transparent strain sensors that can be applicable to wireless health monitoring devices. The CN hydrogel is composed of polyacrylamide incorporated with CNT bridged LM (eutectic gallium-indium). The addition of CNT bridged LM as a conductive filler provided the advantages of metal-based CN hydrogels and carbon-based CN hydrogels. Consequently, it showed high electrical conductivity (94 S m^{-1}), stretchability (2,200%), transparency (93%), adhesion (20 kPa) and self-healing property. In addition, gauge factors of 4.8 and 12.7 were achieved at applied strains lower than 200% and higher than 200%, respectively. When the LM/CNT CN hydrogels were implanted on the heart and tail of Chinese sturgeon, they could sensitively detect movements through electric signals (Fig. 10(a)) [134].

1-4. Electronics Based on Hydrogels with Conductive Coating

Hydrogels with conductive coatings (CC hydrogels) have demonstrated important applications in soft electronics and energy storage devices (supercapacitor and battery) [79,141,182,183]. Considering the high Young's modulus of the components in conventional electronic and energy storage devices, the use of hydrogels allows for the realization of devices with mechanical properties, similar to those of biological tissues.

Hao et al. reported that a CC hydrogel-based soft electronics that can monitor the motion of animal (rice field eel) and heart with an aid of self-morphing function [141]. The CC hydrogel was fabricated by LM amalgam (eutectic gallium indium (EGaIn) alloy doped with Ni particles) assembled on hydrogel surface (poly(acrylamide-co-methacrylic acid)) by stencil printing. The prepared hydrogel device presented high electrical conductivity (10^5 S m^{-1}) and stretchability (>600%) as well as self-morphing functions. The active self-morphing was enabled by gradient structures of internal stress, resulting in facile conformal contact with 3-dimensional surfaces of organs. Based on the record of resistance changes with conformal contacts on biological tissue, diverse motions of the rice field eel and replicated beating of the rabbit heart were successfully monitored with CC hydrogel-based devices.

Ye et al. reported a PAM/CNT conductive hydrogel coated on both faces of PAM/LiCl hydrogel and PAM/zinc trifluoromethanesulfonate ($Zn(OTf)_2$) hydrogel electrolytes [183]. The prepared PAM/CNT-based CC electrodes demonstrated substantial electrical conductivity with rapid charge transfer at the interfaces based on the interfacial dry crosslinking method. When a lithium ion battery device was constructed by sandwiching between PAM/CNT-LMO ($LiMn_2O_4$ (LMO) loaded hydrogel electrode) and PAM/CNT-LTP ($LiTi_2(PO_4)_3$ (LTP) loaded hydrogel electrode), it showed high electrochemical performance of specific capacities of 82 mAh g^{-1}. Moreover, the self-healing functionality can be obtained by additional functional components in the hydrogel electrodes, originating from increased hydrogen bonds.

A multi-responsive healable supercapacitor can also be fabricated by integrating an Fe_3O_4@Au/polyacrylamide (MFP) hydrogel with Ag nanowire films on both sides of the hydrogel (Fig. 10(b)) [79]. The prepared hydrogel supercapacitor exhibited areal capacitance of 1,264 mF cm^{-2} along with stretchability of 1,200%, attributed to high electrical conductivity as well superior mechanical properties. In addition, the large number of dynamic Au-SR coordination bonds, which can trigger the reconstruction of dynamic bonds, enabled stimuli-triggered healing property. Specifically, a magnetic field and near IR laser can induce healing of hydrogel devices with the aid of the photothermal features of Au nanoparticles and the magneto-thermal features of Fe_3O_4 nanoparticles. Thus, a healing efficiency of 86.3% was achieved.

2. Hydrogel-based Robotics

Conventional robots depend primarily on electromagnetic motors or actuators that consist of intrinsically bulky and rigid components. Therefore, many studies have been conducted to develop electroactive soft actuators that exhibit performance and softness similar to those natural muscles. Hydrogel electrodes, which can sustain electrical conductivity at highly deformed states, have played an important role in the development of soft actuators, and consequently, soft robotic systems.

2-1. Hydrogel-based Electrostatic Actuations

Ionic hydrogels can be used to induce significant Maxwell stresses by applying a high voltage at high frequencies. Keplinger et al. reported electrostatic actuators based on integrated structures of elastomers sandwiched between two ionic hydrogels. When an AC voltage is applied to the elastomer through two sandwiched ionic hydrogels, ions with opposite charges accumulate at the interface between the hydrogel and the elastomer. Consequently, this results in the expansion of the elastomer layer due to Maxwell stress induced by the accumulated charges at the interfaces. Because hydrogels are much softer than elastomers, they have little influence on the mechanical deformation of the entire device. In addition, the transparent properties of hydrogels enable the generation of fully transparent artificial muscles that can be used in transparent loudspeaker [35]. Based on an electrostatic working mechanism, Li et al. con-

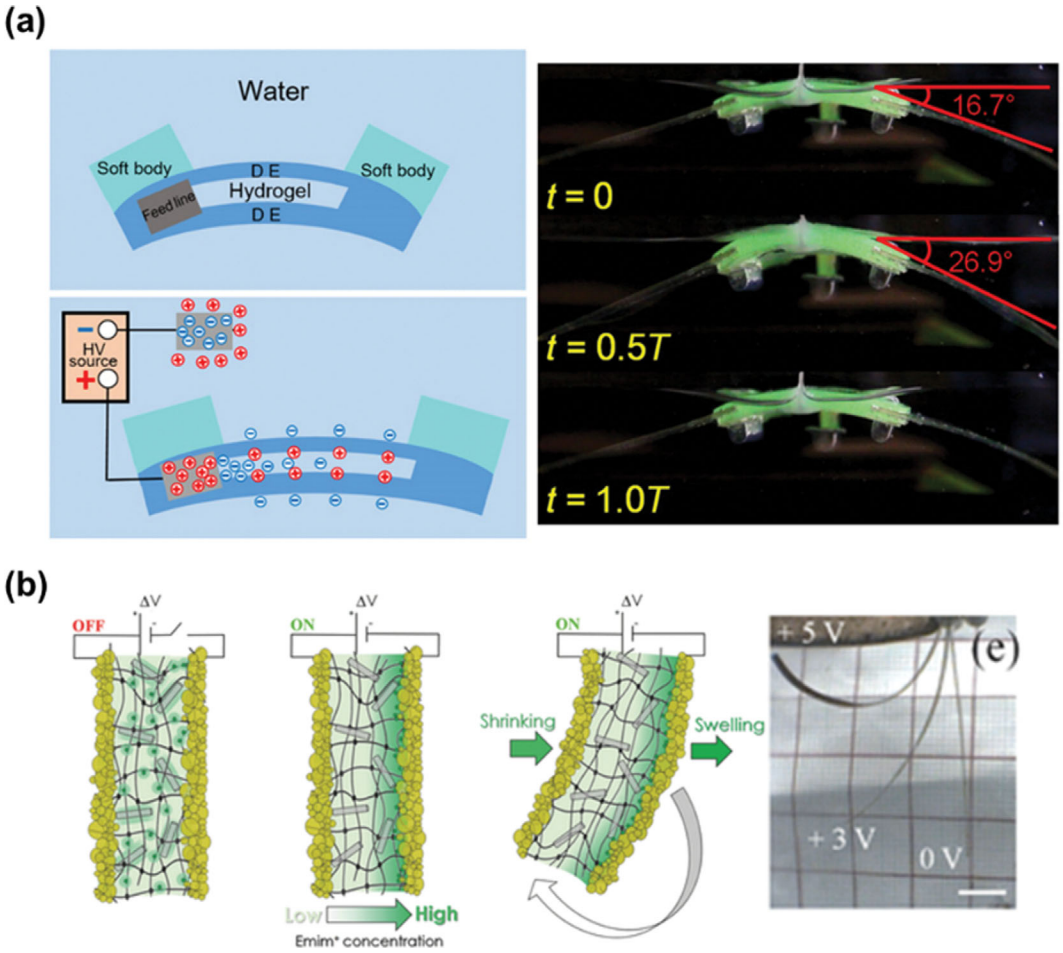

Fig. 11. Robotic applications based on conductive hydrogels. (a) Working mechanism of electrostatic hydrogel actuator and its application into soft electronic fish. Adapted from ref. [184] under the terms of the CC BY-NC, Creative Commons Attribution NonCommercial License 4.0 (https://creativecommons.org/licenses/by-nc/4.0), copyright 2017 AAAS. (b) Working mechanism of electrochemical hydrogel actuator and its actuation at different applied electric potentials. Adapted from ref. [148] with permission from John Wiley and Sons, copyright 2016.

structed a robotic system that can swim in water (0.69 body length per second) with integrated battery and electronic circuits as shown in Fig. 11(a) [184]. In addition to previous studies on plane-structured ionic devices, Lee et al. demonstrated a fiber-shaped ionic device that can integrate the sensing and actuation functions with a single device [185]. The ionic device was composed of an elastomer-coated organogel (polyacrylamide (PAAm) with lithium chloride dissolved in ethylene glycol). By applying AC voltages (a few kVs) to the ionic device, the unique functionalities of electrostatic interaction-based adhesion/vibration and electrostatic induction-based sensing can be realized with same ionic device.

Despite the promising performance of ionic artificial muscles based on solid-state elastomers with ionic hydrogels, they suffered from strict device architecture (pre-stretched elastomers with a rigid frame), electric breakdown, and mechanical degradation, restricting a wide range of practical applications. Hydraulically amplified self-healing electrostatic (HASEL) artificial muscles have been reported based on the hydraulic pressure induced by local electrostatic forces using liquid-state dielectric materials [186-188]. New electrostatic artificial muscles can also be constructed with IC hydrogel electrodes [187], which exhibit outstanding and reliable actuating performances. Transparent, high-speed, and large-strain soft actuators have been successfully developed.

2-2. Hydrogel-based Electrochemical Actuators

The integration of ionically conductive hydrogel with electrode layers on the surface of IC hydrogels has been widely used to develop soft actuators operated by electrochemical reaction-based electro-transduction mechanisms. The actuation of electrochemical actuators primarily depends on the expansion of electrodes by electrochemical reactions (i.e., electric double layer capacitive capacitive and pseudocapacitive reactions) and/or the electrostatic repulsion of attracted ions of different sizes near the electrodes (Fig. 11(b)) [149]. Therefore, the actuators can be operated at low voltages and high speeds. Because the performance of the actuator dominantly depends on the amount of energy stored (i.e., ions) in the electrodes, various electrodes have been introduced to improve the performance.

However, the performance of electrochemical actuators is inherently limited by the electrochemical reactions and electrostatic repulsion of ions that occur near or on the surface of the electrode

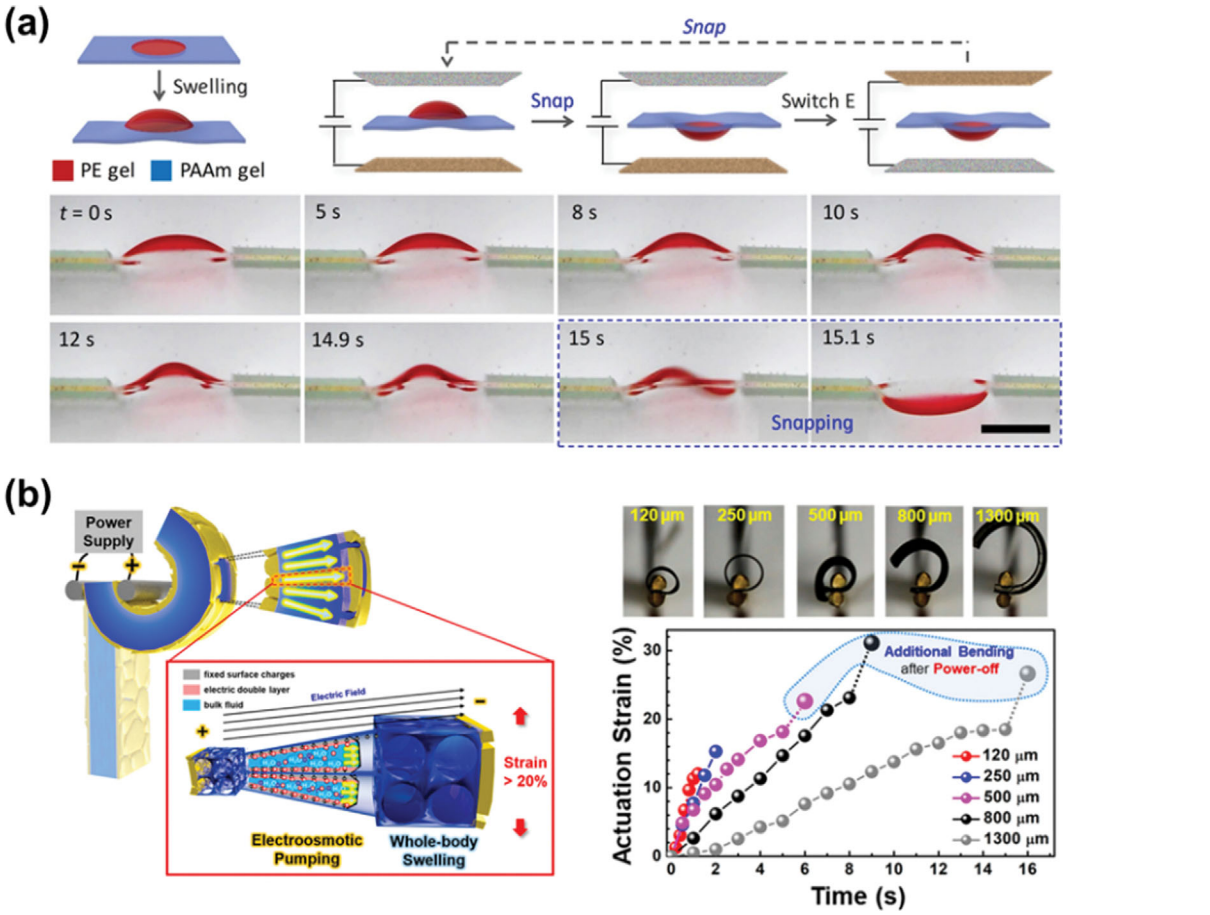

Fig. 12. Robotic applications based on conductive hydrogels. (a) Schematic illustration of electrically-triggered osmosis driven hydrogel actuator based on poly(acrylamide-co-2-acrylamido-2-methylpropanesulfonic acid) and its actuation by applying electric field with remotely positioned electrodes. Adapted from ref. [189] under the terms of the CC BY-NC, Creative Commons Attribution Non-Commercial License 4.0 (https://creativecommons.org/licenses/by-nc/4.0), copyright 2022 AAAS. (b) Schematic illustration of electroosmosis driven hydrogel actuator based on poly(acrylic acid-co-acrylonitile) hydrogel and its actuation by applying electric field through Au coated electrodes. Adapted from ref. [178] with permission from American Chemical Society, copyright 2020.

(typically less than a few μm). Therefore, the actuation strains of the electrochemical actuators were mostly less than 2%, which significantly restricted their actual application in robotic systems. Moreover, efforts to increase the force of the actuators by increasing the thickness of the actuator led to a significantly decreased actuation speed (e.g., 30 s for 1% actuation strain) [148]. Despite these intrinsic limitations, electrochemical actuators have found new opportunities in micro-scale devices, requiring intensive studies to include functional hydrogel for constructing microscale actuating systems.

2-3. Hydrogel-based Electroosmotic Actuators

Previously reported hydrogel actuators have mostly depended on the osmotic pressure-induced swelling/deswelling of polymeric networks in response to various stimuli. However, these hydrogel actuators suffer from slow actuation speeds and poor controllability owing to the inherently slow nature of water diffusion inside the hydrogel matrix. Electrically-triggered osmosis is an effective way of actuating hydrogels by facilitating and accelerating water diffusion in the hydrogel matrix. Li et al. reported the electrically driven actuation of polyelectrolyte hydrogels (poly(acrylamide-co-2-acrylamido-2-methylpropanesulfonic acid)), showing enhanced controllability and performance of actuators in response to an electric field (Fig. 12(a)) [189]. Specifically, the electric field-induced distribution of mobile ions resulted in enhanced water migration, which generated hydrogel swelling. In addition, the use of bi-stable hydrogels leads to a considerably increased response time (i.e., a few seconds) based on snap-through mechanical deformation. In addition to the enhanced actuation speed, hydrogel actuators exhibiting considerably high actuation forces was reported by introducing an electoosmotic mechanism [190]. However, poor consideration of the electrodes (i.e., externally positioned electrodes) resulted in unnecessary electrochemical reactions (operating voltages higher than 5 V) and slow actuation speeds (several minutes), seriously restricting their application in robotic systems.

As described in Section of Fabrication of Hydrogel-Based Electrodes, LbL assembly provides a new versatile method to form highly conductive and mechanically stable electrodes on hydrogels [178, 179]. Specifically, LbL assembly-based interfacial AuNP room temperature sintering process permits to form electrode layers on hydrogel surface, exhibiting substantially high conductivity and stretchability based on unique morphology (wrinkled nanomembrane electrode

(WNE), 4.1×10^4 S cm^{-1} with 110% stretchability) which are essential for the efficient application of an electric field under dynamic conditions in the hydrogel matrix. When an electric field of less than 3 V was applied to the hydrogel through the WNE electrodes, a substantial amount of hydraulic fluid was generated in the hydrogel by electroosmotic pumping, resulting in significant bending motions (strain >30%) (Fig. 12(b)). Based on important breakthroughs in electrode design, the WNE actuators exhibited significantly enhanced efficiency and performance, making them suitable for fast small-scale untethered aquabots far beyond the capability of existing soft actuators. Considering the difficulties in developing small-scale untethered soft robots based on previously reported soft actuators because of the poor performance and/or strict operating conditions of actuators, new mechanism-driven hydrogel actuators can realize insect-scale battery-powered robots based on high performance with low-voltages operating conditions [179].

CONCLUSION AND PERSPECTIVE

In this review, promising approaches for establishing hydrogels as key components in electronic and robotic applications (Table 2) are suggested based on different types of multi-functional hydrogel electrodes. Four distinct hydrogel electrode types are described depending on their fabrication methods along with their applications in various electronic and robotic applications. This section offers an overview by summarizing the distinctive attributes and

Table 2. Electronic and Robotic applications of hydrogel electrodes

Type	Materials	Applications	Features	Ref.
IC hydrogel	PAAm (LiCl)	- Touch panel	- Stretchability ~ 1,000% - Writing/playing music·game	[121]
	PDMS coated PAAm (LiCl)	- Triboelectric nanogenerator - Touch panel	- Output power ~ 4.22 W m^{-2} - Self-clean - Transparent	[50]
	Fiber of coaxial PAAm PDMS with ZnS:Cu	- Luminescent fiber	- Stretchability ~ 250% - 12 cd m^{-2} (5 V μm^{-1} 1 kHz)	[180]
	DE/PAAm(LiCl)/DE	- Soft electronic fish	- Swim at 6.4 cm s^{-1} (0.69 body length s^{-1})	[184]
CP hydrogel	PAA templated PEDET:PSS	- Nerve stimulation - Electrocardiogram recording	- Low stimulating voltage (40 mV, 1 Hz) - SNR ~ 1,009 (60.08 dB)	[129]
	PEDOT:PSS/PU	- Nerve stimulation - Electrocardiogram recording	- Low cytotoxity - High stability	[130]
CN hydrogel	LM/CNT embedded PAAm hydrogel	- Motion sensor	- Self-healing (20 min) - Low detection limit (0.01 mm, 0.25% stretch) - Health monitoring	[134]
	Ag_{flakes}/LM embedded PVA-Borax gel	- Circuit connector - EMG sensor	- Self-healing - Anti-drying - High-signal-to-noise-ratio	[80]
	AgNWs embedded PAAm hydrogel	- Wearable antenna - Supercapacitor	- Stretchable antenna - Capacitance ~ 158.33 mF	[131]
CC hydrogel	LM-printed P(AAm-co-MAAc)	- Motion sensor	- Self-shaping - Good interfacial contact - Animal/organ monitoring	[141]
	MXene-coated Nafion	- Soft actuator - Flower robot	- Capacitance ~ 932 F cm^{-3} - Actuation strain ~ 1.37% - Low operating voltage <1 V - High frequency ~ 20 Hz	[149]
	PAM/CNT electrode coated on PAM	- Soft battery	- Modulus ~ 80 kPa - Capacitance ~ 370 mAh g^{-1}	[183]
	Au NPs assembly on PAA-based hydrogels	- Small-scale aquabot	- Actuation strain >50% - Low operating voltage <3 V - Untethered robots	[179]

challenges of each type of hydrogel electrodes.

The first type is ionic hydrogels, which employ mobile ions dissolved in an aqueous phase as charge carriers in a hydrogel matrix. Although this method can be applied to almost all types of hydrogels, it suffers from an intrinsically low electrical conductivity, which limits its applicability. The second type is conductive polymer-based hydrogels which consist of conducting polymeric networks where charges are transported through π-π interactions. CP hydrogels can achieve higher electrical conductivities than those of ionic hydrogels; however, their conductivities are still low, and only a limited range of these hydrogels can be used. The third type is conductive nanocomposite hydrogels containing additional conductive components inside the hydrogel matrix. This hydrogel type is characterized by a high degree of electrical conductivity. According to previous reports, CN hydrogels suffer from a trade-off between electrical conductivity and mechanical properties, originating from the undesirable effects of conductive components at higher concentrations in the hydrogel matrix. Recently, a new approach has been suggested that allows high electrical conductivity at low concentrations, opening new pathways for this type of hydrogel electrodes. The last type is a conductive layer coated hydrogel comprising metallic or carbonaceous electrode layers on the hydrogel surface. Despite having the highest achievable electrical conductivity compared to other types of hydrogels, CC hydrogels suffer from delamination of the electrode layer under mechanical deformation and compromised mechanical properties, all of which originate from poor interfacial interactions between the conductive components and the hydrogels. However, recently suggested novel LbL-based coating methods permit the formation of robust, compliant, thin, and highly conductive layers on hydrogel surfaces without affecting the mechanical properties of the hydrogel. Moreover, facile application to a variety of hydrogels and the formation of wrinkled and/or porous electrode structures provide the additional capability to impart various functionalities to a wide range of hydrogels. These promising properties of the CC hydrogel electrodes can be successfully applied in various electronic and robotic applications that cannot be realized with previously reported soft electrodes.

Despite the significant achievements in the development of hydrogel electrodes for flexible electronics, several challenges remain to be addressed, requiring continued efforts to further advance knowledge in the field. One of the most important challenges that should be addressed is achieving high electrical conductivity without compromising mechanical properties. In particular, achieving an electrical conductivity comparable to that of bulk metals with tissue-like softness provides new possibilities for various applications, particularly therapeutic electronic and robotic applications. Secondly, more generalizable and universal methods that can be applied to a wider range of hydrogels should be developed. Considerable efforts have been made to develop new types of hydrogels with outstanding properties. Imparting electrical properties to these new hydrogel types can provide new opportunities for electronic and robotic applications. The application of embedding and coating methods to various types of hydrogels with superior mechanical properties and functionalities is desirable. Finally, several undesirable properties must be considered in future studies. Despite the promising properties of hydrogels, their deswelling, dehydration, and freezing phenomena make their use in actual electronic or robotic applications challenging because of the intrinsic nature of hydrogels containing large amounts of water. The incorporation of organic solvents that are involatile or thin layer of coating preventing environmental effects have shown possibilities of overcoming such problems. Therefore, further research is required in the future.

Considering the issues discussed above, hydrogel electrodes will play an essential role in next-generation electronics and robotics, particularly in human-interfaced, -integrated-, and -friendly applications.

ACKNOWLEDGEMENTS

This work was supported by the Gachon University research fund of 2022 (GCU-202300970001) and the National Research Foundation of Korea (NRF) grant funded by the Korea government (MSIT) (No. RS-2023-00244975).

CONFLICT OF INTEREST

The authors declare no conflict of interest.

REFERENCES

1. J. A. Rogers, T. Someya and Y. Huang, *Science*, **327**, 1603 (2010).
2. J. Byun, Y. Lee, J. Yoon, B. Lee, E. Oh, S. Chung, T. Lee, K.-J. Cho, J. Kim and Y. Hong, *Sci. Robot.*, **3**, eaas9020 (2018).
3. Y. Chen, Y. Zhang, Z. Liang, Y. Cao, Z. Han and X. Feng, *npj Flex. Electron.*, **4**, 2 (2020).
4. Y. Park, T. S. Chung, G. Lee and J. A. Rogers, *Chem. Rev.*, **122**, 5277 (2021).
5. S. Liu, Y. Rao, H. Jang, P. Tan and N. Lu, *Matter*, **5**, 1104 (2022).
6. Y. Luo, M. R. Abidian, J. H. Ahn, D. Akinwande, A. M. Andrews, M. Antonietti, Z. Bao, M. Berggren, C. A. Berkey, C. J. Bettinger, J. Chen, P. Chen, W. Cheng, X. Cheng, S. J. Choi, A. Chortos, C. Dagdeviren, R. H. Dauskardt, C. A. di, M. D. Dickey, X. Duan, A. Facchetti, Z. Fan, Y. Fang, J. Feng, X. Feng, H. Gao, W. Gao, X. Gong, C. F. Guo, X. Guo, M. C. Hartel, Z. He, J. S. Ho, Y. Hu, Q. Huang, Y. Huang, F. Huo, M. M. Hussain, A. Javey, U. Jeong, C. Jiang, X. Jiang, J. Kang, D. Karnaushenko, A. Khademhosseini, D. H. Kim, I. D. Kim, D. Kireev, L. Kong, C. Lee, N. E. Lee, P. S. Lee, T. W. Lee, F. Li, J. Li, C. Liang, C. T. Lim, Y. Lin, D. J. Lipomi, J. Liu, K. Liu, N. Liu, R. Liu, Y. Liu, Y. Liu, Z. Liu, Z. Liu, X. J. Loh, N. Lu, Z. Lv, S. Magdassi, G. G. Malliaras, N. Matsuhisa, A. Nathan, S. Niu, J. Pan, C. Pang, Q. Pei, H. Peng, D. Qi, H. Ren, J. A. Rogers, A. Rowe, O. G. Schmidt, T. Sekitani, D. G. Seo, G. Shen, X. Sheng, Q. Shi, T. Someya, Y. Song, E. Stavrinidou, M. Su, X. Sun, K. Takei, X. M. Tao, B. C. K. Tee, A. V. Y. Thean, T. Q. Trung, C. Wan, H. Wang, J. Wang, M. Wang, S. Wang, T. Wang, Z. L. Wang, P. S. Weiss, H. Wen, S. Xu, T. Xu, H. Yan, X. Yan, H. Yang, L. Yang, S. Yang, L. Yin, C. Yu, G. Yu, J. Yu, S. H. Yu, X. Yu, E. Zamburg, H. Zhang, X. Zhang, X. Zhang, X. Zhang, Y. Zhang, Y. Zhang, S. Zhao, X. Zhao, Y. Zheng, Y. Q. Zheng, Z. Zheng, T. Zhou, B. Zhu, M. Zhu, R. Zhu, Y. Zhu, Y. Zhu, G. Zou and X. Chen, *ACS Nano*, **17**, 5211 (2023).
7. S. I. Rich, R. J. Wood and C. Majidi, *Nat. Electron.*, **1**, 102 (2018).
8. W. Kim, J. Byun, J.-K. Kim, W.-Y. Choi, K. Jakobsen, J. Jakobsen,

D.-Y. Lee and K.-J. Cho, *Sci. Robot.*, **4**, eaay3493 (2019).
9. Z. Zhakypov, K. Mori, K. Hosoda and J. Paik, *Nature*, **571**, 381 (2019).
10. J. Byun, M. Park, S.-M. Baek, J. Yoon, W. Kim, B. Lee, Y. Hong and K.-J. Cho, *Sci. Robot.*, **6**, eabe0637 (2021).
11. P. Rothemund, Y. Kim, R. H. Heisser, X. Zhao, R. F. Shepherd and C. Keplinger, *Nat. Mater.*, **20**, 1582 (2021).
12. Y. Kim, J. Zhu, B. Yeom, M. Di Prima, X. Su, J.-G. Kim, S. J. Yoo, C. Uher and N. A. Kotov, *Nature*, **500**, 59 (2013).
13. N. Matsuhisa, D. Inoue, P. Zalar, H. Jin, Y. Matsuba, A. Itoh, T. Yokota, D. Hashizume and T. Someya, *Nat. Mater.*, **16**, 834 (2017).
14. S. Choi, S. I. Han, D. Jung, H. J. Hwang, C. Lim, S. Bae, O. K. Park, C. M. Tschabrunn, M. Lee, S. Y. Bae, J. W. Yu, J. H. Ryu, S.-W. Lee, K. Park, P. M. Kang, W. B. Lee, R. Nezafat, T. Hyeon and D.-H. Kim, *Nat. Nanotechnol.*, **13**, 1048 (2018).
15. E. J. Markvicka, M. D. Bartlett, X. Huang and C. Majidi, *Nat. Mater.*, **17**, 618 (2018).
16. S. Chen, H.-Z. Wang, R.-Q. Zhao, W. Rao and J. Liu, *Matter*, **2**, 1446 (2020).
17. Y. Xu, Y. Su, X. Xu, B. Arends, G. Zhao, D. N. Ackerman, H. Huang, S. P. Reid, J. L. Santarpia, C. Kim, Z. Chen, S. Mahmoud, Y. Ling, A. Brown, Q. Chen, G. Huang, J. Xie and Z. Yang, *Sci. Adv.*, **9**, eadf0575 (2023).
18. C. B. Cooper, S. E. Root, L. Michalek, S. Wu, J.-C. Lai, M. Khatib, S. T. Oyakhire, R. Zhao, J. Qin and Z. Bao, *Science*, **380**, 935 (2023).
19. Y. Jiang, S. Ji, J. Sun, J. Huang, Y. Li, G. Zou, T. Salim, C. Wang, W. Li, H. Jin, J. Xu, S. Wang, T. Lei, X. Yan, W. Y. X. Peh, S.-C. Yen, Z. Liu, M. Yu, H. Zhao, Z. Lu, G. Li, H. Gao, Z. Liu, Z. Bao and X. Chen, *Nature*, **614**, 456 (2023).
20. W. Wang, Y. Jiang, D. Zhong, Z. Zhang, S. Choudhury, J. C. Lai, H. Gong, S. Niu, X. Yan, Y. Zheng, C. C. Shih, R. Ning, Q. Lin, D. Li, Y. H. Kim, J. Kim, Y. X. Wang, C. Zhao, C. Xu, X. Ji, Y. Nishio, H. Lyu, J. B. H. Tok and Z. Bao, *Science*, **380**, 735 (2023).
21. Y. Zheng, L. Michalek, Q. Liu, Y. Wu, H. Kim, P. Sayavong, W. Yu, D. Zhong, C. Zhao, Z. Yu, J. A. Chiong, H. Gong, X. Ji, D. Liu, S. Zhang, N. Prine, Z. Zhang, W. Wang, J. B.-H. Tok, X. Gu, Y. Cui, J. Kang and Z. Bao, *Nat. Nanotechnol.*, **18**, 1175 (2023).
22. H. Lee, H. Li, Y. S. Kim, S. M. Park, D. Lee, S. Lee, H. S. Lee, Y. H. Kim and B. Kang, *Macromol. Rapid Commun.*, **43**, 2200277 (2022).
23. H. Lee, B. Moon, M.-J. Kim, H. S. Kim, D.-H. Hwang, B. Kang and K. Cho, *ACS Appl. Mater. Interfaces*, **14**, 39098 (2022).
24. H. Lee, S. B. Lee, Y.-S. Kim, H. Kim, M.-J. Kim, T. W. Yoon, D. Lee, J. H. Cho, Y.-H. Kim and B. Kang, *Chem. Eng. J.*, **468**, 143654 (2023).
25. J. Ko, R. Berger, H. Lee, H. Yoon, J. Cho and K. Char, *Chem. Soc. Rev.*, **50**, 3585 (2021).
26. C. Yang and Z. Suo, *Nat. Rev. Mater.*, **3**, 125 (2018).
27. H. Yuk, B. Lu and X. Zhao, *Chem. Soc. Rev.*, **48**, 1642 (2019).
28. F. Fu, J. Wang, H. Zeng and J. Yu, *ACS Mater. Lett.*, **2**, 1287 (2020).
29. Q. Yang, Z. Hu and J. A. Rogers, *Accounts Mater. Res.*, **2**, 1010 (2021).
30. V. V. Tran, K. Lee, T. N. Nguyen and D. Lee, *Gels*, **9**, 12 (2022).
31. L. Hu, P. L. Chee, S. Sugiarto, Y. Yu, C. Shi, R. Yan, Z. Yao, X. Shi, J. Zhi, D. Kai, H.-D. Yu and W. Huang, *Adv. Mater.*, **35**, 2205326 (2023).
32. Y. Zhang, Y. Tan, J. Lao, H. Gao and J. Yu, *ACS Nano*, **17**, 9681 (2023).
33. T. Zhu, Y. Ni, G. M. Biesold, Y. Cheng, M. Ge, H. Li, J. Huang, Z. Lin and Y. Lai, *Chem. Soc. Rev.*, **52**, 473 (2023).
34. Y. S. Zhang and A. Khademhosseini, *Science*, **356**, eaaf3627 (2017).
35. C. Keplinger, J.-Y. Sun, C. C. Foo, P. Rothemund, G. M. Whitesides and Z. Suo, *Science*, **341**, 984 (2013).
36. X. Zhao, X. Chen, H. Yuk, S. Lin, X. Liu and G. Parada, *Chem. Rev.*, **121**, 4309 (2021).
37. Z. Han, P. Wang, Y. Lu, Z. Jia, S. Qu and W. Yang, *Sci. Adv.*, **8**, eabl5066 (2022).
38. G. Singh and A. Chanda, *Biomed. Mater.*, **16**, 062004 (2021).
39. J. P. Gong, Y. Katsuyama, T. Kurokawa and Y. Osada, *Adv. Mater.*, **15**, 1155 (2003).
40. W. R. Illeperuma, J.-Y. Sun, Z. Suo and J. J. Vlassak, *Extreme Mech. Lett.*, **1**, 90 (2014).
41. D. Ye, P. Yang, X. Lei, D. Zhang, L. Li, C. Chang, P. Sun and L. Zhang, *Chem. Mater.*, **30**, 5175 (2018).
42. T. Sedlačík and R. Hoogenboom, *Matter*, **4**, 1456 (2021).
43. X. Lin, X. Zhao, C. Xu, L. Wang and Y. Xia, *J. Polym. Sci.*, **60**, 2525 (2022).
44. G. Zhang, J. Kim, S. Hassan and Z. Suo, *Proc. National Acad. Sci.*, **119**, e2203962119 (2022).
45. J. Kim, G. Zhang, M. Shi and Z. Suo, *Science*, **374**, 212 (2021).
46. L. Fu, L. Li, Q. Bian, B. Xue, J. Jin, J. Li, Y. Cao, Q. Jiang and H. Li, *Nature*, **618**, 740 (2023).
47. H. Yuk, T. Zhang, S. Lin, G. A. Parada and X. Zhao, *Nat. Mater.*, **15**, 190 (2016).
48. H. Yuk, T. Zhang, G. A. Parada, X. Liu and X. Zhao, *Nat. Commun.*, **7**, 12028 (2016).
49. D. Wirthl, R. Pichler, M. Drack, G. Kettlguber, R. Moser, R. Gerstmayr, F. Hartmann, E. Bradt, R. Kaltseis, C. M. Siket, S. E. Schausberger, S. Hild, S. Bauer and M. Kaltenbrunner, *Sci. Adv.*, **3**, e1700053 (2017).
50. Y. Lee, S. H. Cha, Y.-W. Kim, D. Choi and J.-Y. Sun, *Nat. Commun.*, **9**, 1804 (2018).
51. Q. Liu, G. Nian, C. Yang, S. Qu and Z. Suo, *Nat. Commun.*, **9**, 846 (2018).
52. B. Xue, J. Gu, L. Li, W. Yu, S. Yin, M. Qin, Q. Jiang, W. Wang and Y. Cao, *Nat. Commun.*, **12**, 7156 (2021).
53. H. Yuk, C. E. Varela, C. S. Nabzdyk, X. Mao, R. F. Padera, E. T. Roche and X. Zhao, *Nature*, **575**, 169 (2019).
54. C. Wang, X. Chen, L. Wang, M. Makihata, H.-C. Liu, T. Zhou and X. Zhao, *Science*, **377**, 517 (2022).
55. J. Wu, H. Yuk, T. L. Sarrafian, C. F. Guo, L. G. Griffiths, C. S. Nabzdyk and X. Zhao, *Sci. Transl. Med.*, **14**, eabh2857 (2022).
56. K. Y. Lee and D. J. Mooney, *Chem. Rev.*, **101**, 1869 (2001).
57. D. Seliktar, *Science*, **336**, 1124 (2012).
58. Y. Zhang and Y. Huang, *Front. Chem.*, **8**, 615665 (2021).
59. H. S. Kim, H.-K. Kwon, D. H. Lee, T. N. Le, H.-J. Park and M. I. Kim, *Int. J. Nanomedicine*, **14**, 8409 (2019).
60. Y. Lee, W. Song and J.-Y. Sun, *Mater. Today Phys.*, **15**, 100258 (2020).
61. H. Kim, W.-G. Koh and H. J. Lee, *React. Funct. Polym.*, **164**, 104933 (2021).
62. C. Wang, T. Yokota and T. Someya, *Chem. Rev.*, **121**, 2109 (2021).
63. Y. Hong, Z. Lin, Y. Yang, T. Jiang, J. Shang and Z. Luo, *Int. J. Mol. Sci.*, **23**, 4578 (2022).

64. M. S. Kong, W.-G. Koh and H. J. Lee, *Gels*, **8**, 214 (2022).
65. M. Baumgartner, F. Hartmann, M. Drack, D. Preninger, D. Wirthl, R. Gerstmayr, L. Lehner, G. Y. Mao, R. Pruckner, S. Demchyshyn, L. Reiter, M. Strobel, T. Stockinger, D. Schiller, S. Kimeswenger, F. Greibich, G. Buchberger, E. Bradt, S. Hild, S. Bauer and M. Kaltenbrunner, *Nat. Mater.*, **19**, 1102 (2020).
66. J. H. Kang, M. H. Turabee, D. S. Lee, Y. J. Kwon and Y. T. Ko, *Biomed. Pharmacother.*, **143**, 112144 (2021).
67. D. L. Taylor and M. in het Panhuis, *Adv. Mater.*, **28**, 9060 (2016).
68. W. Zou, J. Dong, Y. Luo, Q. Zhao and T. Xie, *Adv. Mater.*, **29**, 1606100 (2017).
69. Y. Liu and S.-h. Hsu, *Front. Chem.*, **6**, 449 (2018).
70. J. Hur, K. Im, S. W. Kim, J. Kim, D.-Y. Chung, T.-H. Kim, K. H. Jo, J. H. Hahn, Z. Bao, S. Hwang and N. Park, *ACS Nano*, **8**, 10066 (2014).
71. Y.-K. Li, C.-G. Guo, L. Wang, Y. Xu, C.-y. Liu and C.-Q. Wang, *RSC Adv.*, **4**, 55133 (2014).
72. N. Park, S. C. Chae, I. T. Kim and J. Hur, *J. Nanosci. Nanotechnol.*, **16**, 1400 (2016).
73. M.-M. Iftime, S. Morariu and L. Marin, *Carbohydr. Polym.*, **165**, 39 (2017).
74. G. Singh, G. Singh, K. Damarla, P. K. Sharma, A. Kumar and T. S. Kang, *ACS Sust. Chem. Eng.*, **5**, 6568 (2017).
75. X. P. Hao, C. W. Zhang, X. N. Zhang, L. X. Hou, J. Hu, M. D. Dickey, Q. Zheng and Z. L. Wu, *Small*, **18**, 2201643 (2022).
76. C. Bilici, V. Can, U. Nöchel, M. Behl, A. Lendlein and O. Okay, *Macromolecules*, **49**, 7442 (2016).
77. K. Liu, X. Pan, L. Chen, L. Huang, Y. Ni, J. Liu, S. Cao and H. Wang, *ACS Sust. Chem. Eng.*, **6**, 6395 (2018).
78. W. Yang, B. Shao, T. Liu, Y. Zhang, R. Huang, F. Chen and Q. Fu, *ACS Appl. Mater. Interfaces*, **10**, 8245 (2018).
79. H. Qin, P. Liu, C. Chen, H.-P. Cong and S.-H. Yu, *Nat. Commun.*, **12**, 4297 (2021).
80. Y. Zhao, Y. Ohm, J. Liao, Y. Luo, H.-Y. Cheng, P. Won, P. Roberts, M. R. Carneiro, M. F. Islam, J. H. Ahn, L. M. Walker and C. Majidi, *Nat. Electron.*, **6**, 206 (2023).
81. S. M. Kim, B. Lee, H. Yoon and K.-Y. Suh, *Analyst*, **138**, 6230 (2013).
82. M. Ding, L. Jing, H. Yang, C. Machnicki, X. Fu, K. Li, I. Wong and P.-Y. Chen, *Mater. Today Adv.*, **8**, 100088 (2020).
83. X. Liu, J. Liu, S. Lin and X. Zhao, *Mater. Today*, **36**, 102 (2020).
84. N. Park and J. Kim, *Adv. Intell. Syst.*, **2**, 1900135 (2020).
85. L. Dong, A. K. Agarwal, D. J. Beebe and H. Jiang, *Nature*, **442**, 551 (2006).
86. J. Kim, J. A. Hanna, M. Byun, C. D. Santangelo and R. C. Hayward, *Science*, **335**, 1201 (2012).
87. Y. S. Kim, M. Liu, Y. Ishida, Y. Ebina, M. Osada, T. Sasaki, T. Hikima, M. Takata and T. Aida, *Nat. Mater.*, **14**, 1002 (2015).
88. J. Bae and J. Hur, *Sci. Adv. Mater.*, **8**, 176 (2016).
89. K. H. Son and J. W. Lee, *Materials*, **9**, 854 (2016).
90. H. Lin, S. Ma, B. Yu, M. Cai, Z. Zheng, F. Zhou and W. Liu, *Chem. Mater.*, **31**, 4469 (2019).
91. K. Mo, M. He, X. Cao and C. Chang, *J. Mater. Chem. C*, **8**, 2756 (2020).
92. S. Zhou, B. Wu, Q. Zhou, Y. Jian, X. Le, H. Lu, D. Zhang, J. Zhang, Z. Zhang and T. Chen, *Macromol. Rapid Commun.*, **41**, 1900543 (2020).
93. M. A. Iqbal, T. Akhter, M. Faheem, A. Mahmood, W. Al-Masry, S. Nadeem, S. U. Hassan and C. H. Park, *Cellulose*, **30**, 7519 (2023).
94. H.-W. Kammer, T. Inoue and T. Ougizawa, *Polymer*, **30**, 888 (1989).
95. M. J. Taylor, P. Tomlins and T. S. Sahota, *Gels*, **3**, 4 (2017).
96. M. Heskins and J. E. Guillet, *J. Macromol. Sci.—Chem.*, **2**, 1441 (1968).
97. S.-B. Bae and S.-W. Lee, *J. Nanosci. Nanotechnol.*, **15**, 7962 (2015).
98. G. Kim, Y. Jung, K. Cho, H. J. Lee and W.-G. Koh, *Mater. Sci. Eng.: C*, **115**, 111128 (2020).
99. N. Zhang, M. Liu, Y. Shen, J. Chen, L. Dai and C. Gao, *J. Mater. Sci.*, **46**, 1523 (2011).
100. J. Seuring and S. Agarwal, *Macromol. Rapid Commun.*, **33**, 1898 (2012).
101. Q. Zhang and R. Hoogenboom, *Prog. Polym. Sci.*, **48**, 122 (2015).
102. J. Duan, X. Liang, K. Zhu, J. Guo and L. Zhang, *Soft Matter*, **13**, 345 (2017).
103. Y. Ma, M. Hua, S. Wu, Y. Du, X. Pei, X. Zhu, F. Zhou and X. He, *Sci. Adv.*, **6**, eabd2520 (2020).
104. M. Torres-Lugo and N. A. Peppas, *Macromolecules*, **32**, 6646 (1999).
105. C. M. Schilli, M. Zhang, E. Rizzardo, S. H. Thang, Y. Chong, K. Edwards, G. Karlsson and A. H. Müller, *Macromolecules*, **37**, 7861 (2004).
106. G. Li, G. Zhang, R. Sun and C.-P. Wong, *Polymer*, **107**, 332 (2016).
107. P. Mukhopadhyay, K. Sarkar, S. Bhattacharya, A. Bhattacharyya, R. Mishra and P. P. Kundu, *Carbohydr. Polym.*, **112**, 627 (2014).
108. H. Lee, J. H. Kim, G. Wu, H. M. Lee, J. Kim, D. Kwon, S. Yang, C. K. Kim and H. Yoon, *Adv. Mater. Interfaces*, **5**, 1801142 (2018).
109. C. Lv, X.-C. Sun, H. Xia, Y.-H. Yu, G. Wang, X.-W. Cao, S.-X. Li, Y.-S. Wang, Q.-D. Chen, Y.-D. Yu and H.-B. Sun, *Sens. Actuators B: Chem.*, **259**, 736 (2018).
110. H. Qin, T. Zhang, N. Li, H.-P. Cong and S.-H. Yu, *Nat. Commun.*, **10**, 2202 (2019).
111. A. Kawamura, Y. Hata, T. Miyata and T. Uragami, *Colloids Surf. B: Biointerfaces*, **99**, 74 (2012).
112. A. Cangialosi, C. Yoon, J. Liu, Q. Huang, J. Guo, T. D. Nguyen, D. H. Gracias and R. Schulman, *Science*, **357**, 1126 (2017).
113. X. Qian, Y. Zhao, Y. Alsaid, X. Wang, M. Hua, T. Galy, H. Gopalakrishna, Y. Yang, J. Cui, N. Liu, M. Marszewski, L. Pilon, H. Jiang and X. He, *Nat. Nanotechnol.*, **14**, 1048 (2019).
114. Y. Zhao, C.-Y. Lo, L. Ruan, C.-H. Pi, C. Kim, Y. Alsaid, I. Frenkel, R. Rico, T.-C. Tsao and X. He, *Sci. Robot.*, **6**, eabd5483 (2021).
115. W. Francis, A. Dunne, C. Delaney, L. Florea and D. Diamond, *Sens. Actuators B: Chem.*, **250**, 608 (2017).
116. K. Homma, A. C. Chang, S. Yamamoto, R. Tamate, T. Ueki and J. Nakanishi, *Acta Biomaterialia*, **132**, 103 (2021).
117. J. Gong, N. Komatsu, T. Nitta and Y. Osada, *J. Phys. Chem. B*, **101**, 740 (1997).
118. S. Zhao, P. Tseng, J. Grasman, Y. Wang, W. Li, B. Napier, B. Yavuz, Y. Chen, L. Howell, J. Rincon, F. G. Omenetto and D. L. Kaplan, *Adv. Mater.*, **30**, 1800598 (2018).
119. J. Yeom, A. Choe, S. Lim, Y. Lee, S. Na and H. Ko, *Sci. Adv.*, **6**, eaba5785 (2020).
120. S. Wang, L. Yu, S. Wang, L. Zhang, L. Chen, X. Xu, Z. Song, H. Liu and C. Chen, *Nat. Commun.*, **13**, 3408 (2022).
121. C.-C. Kim, H.-H. Lee, K.H. Oh and J.-Y. Sun, *Science*, **353**, 682

(2016).
122. L. Pan, G. Yu, D. Zhai, H. R. Lee, W. Zhao, N. Liu, H. Wang, B. C.-K. Tee, Y. Shi, Y. Cui and Z. Bao, *Proc. National Acad. Sci.*, **109**, 9287 (2012).
123. Y. Lu, W. He, T. Cao, H. Guo, Y. Zhang, Q. Li, Z. Shao, Y. Cui and X. Zhang, *Sci. Rep.*, **4**, 5792 (2014).
124. B. Yao, H. Wang, Q. Zhou, M. Wu, M. Zhang, C. Li and G. Shi, *Adv. Mater.*, **29**, 1700974 (2017).
125. S. Liang, Y. Zhang, H. Wang, Z. Xu, J. Chen, R. Bao, B. Tan, Y. Cui, G. Fan, W. Wang, W. Wang and W. Liu, *Adv. Mater.*, **30**, 1704235 (2018).
126. B. Lu, H. Yuk, S. Lin, N. Jian, K. Qu, J. Xu and X. Zhao, *Nat. Commun.*, **10**, 1043 (2019).
127. T. Wu, C. Cui, Y. Huang, Y. Liu, C. Fan, X. Han, Y. Yang, Z. Xu, B. Liu, G. Fan and W. Liu, *ACS Appl. Mater. Interfaces*, **12**, 2039 (2019).
128. S. Noh, H. Y. Gong, H. J. Lee and W.-G. Koh, *Materials*, **14**, 308 (2021).
129. J. Chong, C. Sung, K. S. Nam, T. Kang, H. Kim, H. Lee, H. Park, S. Park and J. Kang, *Nat. Commun.*, **14**, 2206 (2023).
130. T. Zhou, H. Yuk, F. Hu, J. Wu, F. Tian, H. Roh, Z. Shen, G. Gu, J. Xu, B. Lu and X. Zhao, *Nat. Mater.*, **22**, 895 (2023).
131. C. Lim, Y. Shin, J. Jung, J. H. Kim, S. Lee and D.-H. Kim, *APL Mater.*, **7**, 031502 (2019).
132. K. S. Kumar, L. Zhang, M. S. Kalairaj, H. Banerjee, X. Xiao, C. C. Jiayi, H. Huang, C. M. Lim, J. Ouyang and H. Ren, *ACS Appl. Mater. Interfaces*, **13**, 37816 (2021).
133. Y. Ohm, C. Pan, M. J. Ford, X. Huang, J. Liao and C. Majidi, *Nat. Electron.*, **4**, 185 (2021).
134. M. Sun, P. Li, H. Qin, N. Liu, H. Ma, Z. Zhang, J. Li, B. Lu, X. Pan and L. Wu, *Chem. Eng. J.*, **454**, 140459 (2023).
135. L. Zhang and G. Shi, *J. Phys. Chem. C*, **115**, 17206 (2011).
136. J. Wu, Q. e. Zhang, A. a. Zhou, Z. Huang, H. Bai and L. Li, *Adv. Mater.*, **28**, 10211 (2016).
137. P. Li, Z. Jin, L. Peng, F. Zhao, D. Xiao, Y. Jin and G. Yu, *Adv. Mater.*, **30**, 1800124 (2018).
138. L. Ye, H. Ji, J. Liu, C. H. Tu, M. Kappl, K. Koynov, J. Vogt and H. J. Butt, *Adv. Mater.*, **33**, 2102981 (2021).
139. W. Zhao, J. Cao, F. Wang, F. Tian, W. Zheng, Y. Bao, K. Zhang, Z. Zhang, J. Yu, J. Xu, X. Liu and B. Lu, *Polymers*, **14**, 1992 (2022).
140. R. H. Hurt, M. Monthioux and A. Kane, *Carbon*, **44**, 1028 (2006).
141. X. P. Hao, C. Y. Li, C. W. Zhang, M. Du, Z. Ying, Q. Zheng and Z. L. Wu, *Adv. Funct. Mater.*, **31**, 2105481 (2021).
142. I.-W. P. Chen, M.-C. Yang, C.-H. Yang, D.-X. Zhong, M.-C. Hsu and Y. Chen, *ACS Appl. Mater. Interfaces*, **9**, 5550 (2017).
143. G. Wu, X. Wu, Y. Xu, H. Cheng, J. Meng, Q. Yu, X. Shi, K. Zhang, W. Chen and S. Chen, *Adv. Mater.*, **31**, 1806492 (2019).
144. Y. Li, N. Li, W. Liu, A. Prominski, S. Kang, Y. Dai, Y. Liu, H. Hu, S. Wai, S. Dai, Z. Cheng, Q. Su, P. Cheng, C. Wei, L. Jin, J. A. Hubbell, B. Tian and S. Wang, *Nat. Commun.*, **14**, 4488 (2023).
145. H. S. Wang, J. Cho, D. S. Song, J. H. Jang, J. Y. Jho and J. H. Park, *ACS Appl. Mater. Interfaces*, **9**, 21998 (2017).
146. S. Ma, Y. Zhang, Y. Liang, L. Ren, W. Tian and L. Ren, *Adv. Funct. Mater.*, **30**, 1908508 (2020).
147. H. Zhang, Z. Lin, Y. Hu, S. Ma, Y. Liang, L. Ren and L. Ren, *Adv. Sci.*, **10**, 2206135 (2023).
148. Y. Yan, T. Santaniello, L. G. Bettini, C. Minnai, A. Bellacicca, R. Porotti, I. Denti, G. Faraone, M. Merlini, C. Lenardi and P. Milani, *Adv. Mater.*, **29**, 1606109 (2017).
149. S. Umrao, R. Tabassian, J. Kim, V. H. Nguyen, Q. Zhou, S. Nam and I.-K. Oh, *Sci. Robot.*, **4**, eaaw7797 (2019).
150. M. Kotal, J. Kim, R. Tabassian, S. Roy, V. H. Nguyen, N. Koratkar and I. K. Oh, *Adv. Funct. Mater.*, **28**, 1802464 (2018).
151. G. Decher and J. D. Hong, *Makromolekulare Chemie. Macromolecular Symposia*, Wiley Online Library, 321 (1991).
152. G. Decher, J. D. Hong and J. Schmitt, *Thin Solid Films*, **210**, 831 (1992).
153. G. Decher, *Science*, **277**, 1232 (1997).
154. F. Caruso, R. A. Caruso and H. Möhwald, *Science*, **282**, 1111 (1998).
155. J. A. Hiller, J. D. Mendelsohn and M. F. Rubner, *Nat. Mater.*, **1**, 59 (2002).
156. J.-S. Lee, J. Cho, C. Lee, I. Kim, J. Park, Y.-M. Kim, H. Shin, J. Lee and F. Caruso, *Nat. Nanotechnol.*, **2**, 790 (2007).
157. J. F. Quinn, A. P. R. Johnston, G. K. Such, A. N. Zelikin and F. Caruso, *Chem. Soc. Rev.*, **36**, 707 (2007).
158. G. K. Such, A. P. R. Johnston and F. Caruso, *Chem. Soc. Rev.*, **40**, 19 (2010).
159. Y. Ko, Y. Kim, H. Baek and J. Cho, *ACS Nano*, **5**, 9918 (2011).
160. J. J. Richardson, J. Cui, M. Björnmalm, J. A. Braunger, H. Ejima and F. Caruso, *Chem. Rev.*, **116**, 14828 (2016).
161. Y. Ko, M. Kwon, W. K. Bae, B. Lee, S. W. Lee and J. Cho, *Nat. Commun.*, **8**, 1 (2017).
162. C. H. Kwon, Y. Ko, D. Shin, M. Kwon, J. Park, W. K. Bae, S. W. Lee and J. Cho, *Nat. Commun.*, **9**, 1 (2018).
163. S. T. Dubas, T. R. Farhat and J. B. Schlenoff, *J. Am. Chem. Soc.*, **123**, 5368 (2001).
164. S. W. Lee, B.-S. Kim, S. Chen, Y. Shao-Horn and P. T. Hammond, *J. Am. Chem. Soc.*, **131**, 671 (2009).
165. Y. Wang, L. Hosta-Rigau, H. Lomas and F. Caruso, *Phys. Chem. Chem. Phys.*, **13**, 4782 (2011).
166. Y. Ko, H. Baek, Y. Kim, M. Yoon and J. Cho, *ACS Nano*, **7**, 143 (2013).
167. M. Yoon, J. Choi and J. Cho, *Chem. Mater.*, **25**, 1735 (2013).
168. M. Park, Y. Kim, Y. Ko, S. Cheong, S. W. Ryu and J. Cho, *J. Am. Chem. Soc.*, **136**, 17213 (2014).
169. Y. Ko, D. Shin, B. Koo, S. W. Lee, W.-S. Yoon and J. Cho, *Nano Energy*, **12**, 612 (2015).
170. T. Ogoshi, S. Takashima and T.-a. Yamagishi, *J. Am. Chem. Soc.*, **137**, 10962 (2015).
171. C. Kim, H. An, A. Jung and B. Yeom, *J. Colloid Interface Sci.*, **493**, 371 (2017).
172. J. Choi, D. Nam, D. Shin, Y. Song, C. H. Kwon, I. Cho, S. W. Lee and J. Cho, *ACS Nano*, **13**, 12719 (2019).
173. Y. Song, D. Kim, S. Kang, Y. Ko, J. Ko, J. Huh, Y. Ko, S. W. Lee and J. Cho, *Adv. Funct. Mater.*, **29**, 1806584 (2019).
174. I. Cho, Y. Song, S. Cheong, Y. Kim and J. Cho, *Small*, **16**, 1906768 (2020).
175. S. Lee, Y. Song, Y. Ko, Y. Ko, J. Ko, C. H. Kwon, J. Huh, S. W. Kim, B. Yeom and J. Cho, *Adv. Mater.*, **32**, 1906460 (2020).
176. M. Kwon, D. Nam, S. Lee, Y. Kim, B. Yeom, J. H. Moon, S. W. Lee, Y. Ko and J. Cho, *Adv. Energy Mater.*, **11**, 2101631 (2021).
177. D. Nam, M. Kwon, Y. Ko, J. Huh, S. W. Lee and J. Cho, *Appl.*

Phys. Rev., **8**, 029901 (2021).
178. J. Ko, D. Kim, Y. Song, S. Lee, M. Kwon, S. Han, D. Kang, Y. Kim, J. Huh, J.-S. Koh and J. Cho, *ACS Nano*, **14**, 11906 (2020).
179. J. Ko, C. Kim, D. Kim, Y. Song, S. Lee, B. Yeom, J. Huh, S. Han, D. Kang, J.-S. Koh and J. Cho, *Sci. Robot.*, **7**, eabo6463 (2022).
180. C. Yang, S. Cheng, X. Yao, G. Nian, Q. Liu and Z. Suo, *Adv. Mater.*, **32**, 2005545 (2020).
181. H. Tian, C. Wang, Y. Chen, L. Zheng, H. Jing, L. Xu, X. Wang, Y. Liu and J. Hao, *Sci. Adv.*, **9**, eadd6950 (2023).
182. S. Lin, H. Yuk, T. Zhang, G. A. Parada, H. Koo, C. Yu and X. Zhao, *Adv. Mater.*, **28**, 4497 (2016).
183. T. Ye, J. Wang, Y. Jiao, L. Li, E. He, L. Wang, Y. Li, Y. Yun, D. Li, J. Lu, H. Chen, Q. Li, F. Li, R. Gao, H. Peng and Y. Zhang, *Adv. Mater.*, **34**, 2105120 (2022).
184. T. Li, G. Li, Y. Liang, T. Cheng, J. Dai, X. Yang, B. Liu, Z. Zeng, Z. Huang and Y. Luo, *Sci. Adv.*, **3**, e1602045 (2017).
185. Y. Lee, W. J. Song, Y. Jung, H. Yoo, M.-Y. Kim, H.-Y. Kim and J.-Y. Sun, *Sci. Robot.*, **5**, eaaz5405 (2020).
186. E. Acome, S. K. Mitchell, T. Morrissey, M. Emmett, C. Benjamin, M. King, M. Radakovitz and C. Keplinger, *Science*, **359**, 61 (2018).
187. N. Kellaris, V. Gopaluni Venkata, G. M. Smith, S. K. Mitchell and C. Keplinger, *Sci. Robot.*, **3**, eaar3276 (2018).
188. P. Rothemund, N. Kellaris, S. K. Mitchell, E. Acome and C. Keplinger, *Adv. Mater.*, **33**, 2003375 (2021).
189. C. Y. Li, S. Y. Zheng, X. P. Hao, W. Hong, Q. Zheng and Z. L. Wu, *Sci. Adv.*, **8**, eabm9608 (2022).
190. H. Na, Y.-W. Kang, C. S. Park, S. Jung, H.-Y. Kim and J.-Y. Sun, *Science*, **376**, 301 (2022).